AFCRL-67-0034

THRESHOLD DETECTION OF GEODETIC SATELLITE IMAGES

by

Sumner Ackerman

EG&G, INC.
Crosby Drive, Bedford, Massachusetts

Contract No. AF 19(628)-5516

Project No. 7600

Task No. 760006

Scientific Report No. 3

Date of Report

21 November 1966

(CONTRACT MONITOR: Robert L. Iliff)

Prepared

for

AIR FORCE CAMBRIDGE RESEARCH LABORATORIES
OFFICE OF AEROSPACE RESEARCH
UNITED STATES AIR FORCE
BEDFORD, MASSACHUSETTS

AFCRL-67-0034

TH ⟨ESHOLD DETECTION
OF
GEODETIC SATELLITE IMAGES

by

Sumner Ackerman

EG&G, INC.
Crosby Drive, Bedford, Massachusetts

Contract No. AF 19(628)-5516

Project No. 7600

Task No. 760006

Scientific Report No. 3

Date of Report

21 November 1966

(CONTRACT MONITOR: Robert L. Iliff)

Prepared

for

AIR FORCE CAMBRIDGE RESEARCH LABORATORIES
OFFICE OF AEROSPACE RESEARCH
UNITED STATES AIR FORCE
BEDFORD, MASSACHUSETTS

ABSTRACT

A literature survey and study has been made on the photographic detection of stellar images. Photographic detection theory in the literature has been extended as required by the special conditions of geodetic satellite photography. These conditions include the optical and temporal characteristics of the laser illumination, the optical roughness of the satellite reflector, and the quality of detection desired.

Experimental work was conducted to determine the energy requirements and the intrinsic location error for threshold images on Type 103-F emulsion. The energy required was found to be 1.5×10^5 to 4.5×10^5 photons at 6940Å; the lower figure applied to objective detection with a microdensitometer having an aperture area equal to the nominal area of the image and requires optimum pre-exposure of the emulsion. The minimum rms location error varies from about 0.5 micron for well-exposed images (exposed over an area of 50-microns diameter) to 2 microns for threshold images.

Failure of the reciprocity law, the effect of intermittent exposure, and scintillation due to the optically rough reflector are not significant. The basic results obtained for emulsion Type 103-F apply essentially to spectroscopic emulsions Types 1-N and 103a-U also.

LIST OF CONTRIBUTORS

Sumner Ackerman, Scientific Specialist, EG&G, Inc., Bedford, Mass.

Thomas S. Morrison, Senior Engineer, EG&G, Inc., Bedford, Mass.

Conrad Gozewski, Engineering Assistant, EG&G, Inc., Bedford, Mass.

Itek Corp., Lexington, Mass.

RELATED CONTRACTS AND PUBLICATIONS

PREVIOUS OR RELATED CONTRACTS

1. Contract No. AF 19(628)-2950 (Experimental Geodetic Laser System)

2. Contract No. AF 19(628)-5516 (Design Study of Advanced Geodetic Laser System)

PREVIOUSLY PRODUCED PUBLICATIONS

1. Ackerman, Sumner, "High Energy Laser System for Geodetic Research," Final Report, AFCRL-65-671, 30 Sept. 1965 (Contract No. AF 19(628)-2950, Items 1 through 9).

2. Ziffer, G. F., and Maxwell, J. P., "Control Unit for Advanced Geodetic Laser System", Report No. B-3364, EG&G, Inc., Bedford, Mass., 11 August 1966.

3. Ackerman, Sumner, "Design Study of Advanced Geodetic Laser System," Scientific Report No. 1, AFCRL-66-731, 30 Sept. 1966 (Contract No. AF 19(628)-5516, Item 3).

4. Ackerman, S., and Morrison, T. S., "Study of a Multi-Pulse Laser Range Finder," Scientific Report No. 2, AFCRL-66-755, 20 October 1966 (Contract No. AF 19(628)-5516, Item 2).

5. Ackerman, S., Morrison, T. S., and Iliff, R. L., "A Programmed Multi-Pulse Range Measurement System," Journal of Applied Optics (to be published).

TABLE OF CONTENTS

SECTION 1

INTRODUCTION

1.1 PURPOSE

The photographic detection of small images has been investigated in depth from numerous points of view. In a geodetic laser system, an assembly of cube corner reflectors is illuminated by a ground-based laser at distances typically in excess of 1000 km and the unresolved image s recorded against a calibration star field by an adjacent, ground-based camera. The laser output energy requirements must be determined for the design of the system. The special incentives for carefully considering the detection principles involved (and within the context of the Geodetic Laser System) are the technical difficulties and the costs associated with the generation of large laser output energies in short intervals of time.

The purpose of this study is to apply the pertinent detection theory that is available to the particular problem of detecting the photographic image of a laser-illuminated satellite, and to extend the theory as required by the conditions that are peculiar to this application. These special conditions include the optical and temporal characteristics of the illumination, the optical "roughness" of the target, and the quality of detection desired.

1.2 SCOPE

This report describes the work performed by EG&G, Inc., under Contract No. AF 19(628)-5516, Item 1, which calls for the contractor to "perform a photographic emulsion study to determine the optimum emulsion and detection techniques for laser satellite geodesy....." and includes:

(1) A literature survey of photographic detection, with emphasis on the threshold detection of stellar images.

(2) Experimental evaluation of several spectroscopic emulsions of the kind currently used in optical satellite geodesy.

(3) Study of reciprocity effect for test emulsions at very low exposure levels.

In addition, the effect on detection of scintillation due to the optically rough target was investigated.

Only one emulsion is quantitatively investigated in detail herein; the characteristics of other emulsions may be described in the Final Report on this contract.

Emphasis is on the unambiguous detection of the satellite image presence; the location of the satellite image is considered briefly in sub-sections 2.5 and 3.3.4.

SECTION 2

THEORETICAL STUDY

2.1 PHOTOGRAPHIC DETECTION, LITERATURE SURVEY

Much of the early work on photographic theory, from the early 1900's through the 1930's, was concerned with the mechanism by which exposed grains in the emulsion, usually crystals of a silver halide, were caused to be developed, that is converted to silver. Einstein's theory of photoelectric emission required energy many orders of magnitude greater than was actually required to make a grain developable. The formation of the developed image was quickly recognized as a catalytic process, whereby the reduction of a relatively few silver ions due to photoelectric emission renders a grain developable in the sense that the entire grain is reduced to silver by the developer more readily than those grains not exposed. (1)(2)(3a)(4a)†

Naturally, much effort was devoted to the question of how much energy is required to make one grain (on the average) developable. This would be comparable to determining the quantum efficiency of a photocathode (average number of photoelectrons emitted per incident photon) which so simply and conveniently describes the sensitivity of phototubes and other photodetectors. Experiments performed with the electron microscope appear to verify the theory that grains can be more or less sensitive, depending on structural imperfections of the grain crystal and impurities which favor the formation of "grain nucleae" or "development centers" of silver atoms(3a). The grain is more easily developed as the number or size of these development centers on the grain surface increases; furthermore, the larger a center, the greater the probability that it will become progressively larger. The movement of silver atoms to development centers and the probability of their oxidation by free halide gas suggest a temporal influence on latent image formation. These theories, with various modifications, explained otherwise anomalous phenomena associated with the photographic process such as the failure of the reciprocity law, solarization, and the Clayden and Herchel effects. (3b)(4b)

---

† Superscript numerals in parentheses refer to similarly numbered entries in the list of references.

Mathematical models of latent image formation were developed, partly to determine the applicability of the quantum efficiency concept. The assumption is generally made that grain exposure is described by Poisson statistics, so that

$$P(r) = \sum_{r=R}^{\infty} \frac{\bar{n}^r}{r!} \exp\left[-\bar{n}\right] \qquad (1)$$

See list of references. (3b)(4c)(5)(6)(7)(8)(9)

P(r) is the probability that a grain is made developable when this requires at least R photons; $\bar{n}$ is the average exposure in photons/grain area. If N_o is the total number of grains in the exposed area, $N_o P(r)$ is the expected number of grains made developable by $\bar{n}$. Equation 1 can be made to conform reasonably well to the shape of experimentally measured D-H curves when R is made small, between 1 and 4. Such small values of R, however, are not in agreement with experimental data which indicates that R can be of the order of hundreds of photons or more. This difficulty may be resolved [6] by allowing for a wide range of grain sensitivities within an emulsion and for the failure of grains to absorb or utilize all the incident photons for various reasons, so that [9]

$$P_{RiQ}(r) = \sum_{i=1}^{\infty} Q_i \sum_{r=R_i}^{\infty} \frac{(\bar{n}\,Q)^r}{r!} \exp\left(-\bar{n}\,Q\right) \qquad (2)$$

Q_i is some fraction of the grain population that requires at least R_i photons to be made developable and only a fraction, Q, of the incident photons are actually absorbed. Equation 2 can be made to approximate an experimental D-H curve with R_i covering two or more orders of magnitude.† However, the values of Q, Q_i, and R_i are not unique for a given emulsion; also, R_i is a variable influenced by exposure history.

† Zweig [9] shows that this large range of grain sensitivity is fortuitous for the most common photographic application where the nature of the object results in a wide latitude of exposure.

Thus, the values of Q, Q_i, and R_i are "forcing" a fit to experimental data and are compensating for phenomena peculiar to the photographic process such as the wasting of photons on grains already made developable. R_i, in this context, is the necessary, not the sufficient number of photons required for development. Equation 2, and similar relationships, demonstrates a statistical mechanism accounting for the general configuration of the D-H function and shows that quantum efficiency, in the usual sense, cannot be used to characterize the sensitivity of photographic emulsions. Due to the complexity and non-linearity of photographic detectors, our approach to photographic detection must be confined to the use of experimentally measured characteristic functions of emulsions† and their statistical properties.

The information in the photographic plate can be extracted by scanning along two coordinates, x and y, and measuring the optical density or the number of developed grains within an appropriate scanning area, a. $D(x, y)_a$ or $N(x, y)_a$ are random functions due to noise or a combination of noise and signal. Random noise generally consists of grains developed due to pre-exposure†† of the emulsion (fog) and background illumination. The noise can be described in terms of its standard deviation, $\sigma_a(\bar{D})$ or $\sigma_a(\bar{N})$. An increment of energy density, ΔM^*, photons/unit area, is defined as the exposure required for an incremental change in density (or grain count) equal to $\sigma_a(\bar{D})$. Zweig, et al [10a], define ($a\,\Delta M^*$) as the "least detectable energy", or the "noise equivalent energy", Δ_μ:

$$\Delta_\mu = a\,\Delta M^* \quad \text{photons} \tag{3}$$

and a quantity, termed "sensitivity,"

$$S = \frac{1}{\Delta_\mu} = \frac{g}{a\,\sigma_a(\bar{D})} \quad \text{photons}^{-1} \tag{4}$$

where g is the slope of the measured characteristic function, $\Delta D/\Delta M$ (Fig. 1), and

$$\Delta M^* \cong \sigma_a(\bar{D})/g$$

† Density, or number of developed grains per unit area, as a function of exposure.

†† Intentional and/or otherwise.

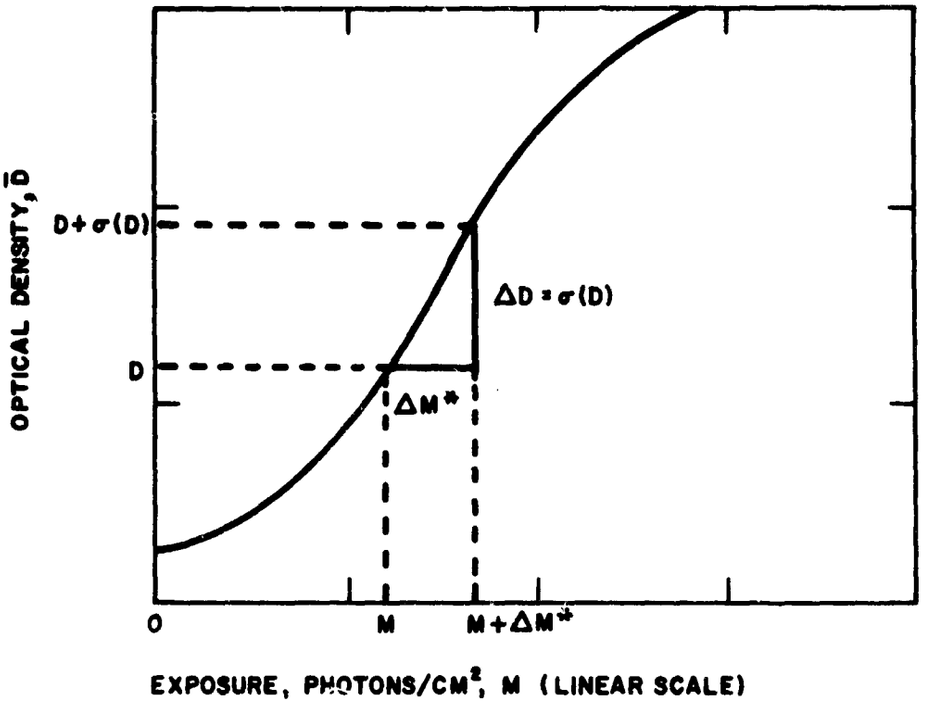

Fig. 1. Typical characteristic curve of a photographic emulsion.

Over the range of scanning areas where

$$\text{Selwyn granularity function} \approx \sigma_a(\bar{D})\sqrt{a} = \text{const.} \tag{5a}$$

(see list of references) (3c)(11)(12)

$$\sigma_a(\bar{D}) \approx \frac{1}{\sqrt{a}} \tag{5b}$$

and

$$S \approx \frac{g}{\sqrt{a}} \tag{5c}$$

Equation 5 is valid over a range of image diameters from a few microns to several hundred microns.

This result can also be obtained by considering the relationship between grain count and density [10, 19]

$$G = \frac{\bar{D}}{0.434\,\alpha} \quad \text{grains/unit area} \tag{6}$$

where G is the developed grain count density, $\bar{D}$ is the average optical density, and α is the area of a grain.

In an area, a

$$aG = \frac{\bar{D}\,a}{0.434\,\alpha} \quad \text{grains}$$

If the number of grains in the area, a, have a Poisson distribution, as the statistics of photographic detection indicates they would have,

$$\sigma\,(aG) = \left[\frac{\bar{D}\,a}{0.434\,\alpha}\right]^{1/2} \tag{7}$$

and

$$\sigma_a\,(\bar{D}) = \left(0.434\bar{D}\,\frac{\alpha}{a}\right)^{1/2} \tag{8}$$

Apparently Equations 8 and 5a are valid for areas where α is, in effect, a constant.

Another quantity, called informational sensitivity[10], I, is the limit of sensitivity when the scanning area is equal to that of the emulsion spread function at 1/4 of peak relative intensity.[3d][10b][12b] Then $a \longrightarrow s$ and

$$I = S_{limit} = \frac{g}{s\,\sigma_s\,(\bar{D})} \tag{9}$$

If it is possible to choose the operating point, $(M, \bar{D})$, then it should be chosen where S has its maximum value. This requires an a-priori knowledge of exposure to background illumination plus knowledge and control over pre-exposure. This knowledge and control exists under

the usual conditions of satellite geodesy. The concept of emulsion sensitivity is particularly useful under such circumstances to obtain the optimum detection efficiency that the emulsion is capable of. Informational sensitivity has been evaluated for a number of commonly used emulsions[10]. The results of particular interest here are that the sensitometric speed of an emulsion alone[3e] does not always indicate the best detectivity; however, a very fast and coarse grain emulsion such as Royal-X will probably detect the smallest number of photons with wavelengths in its spectral bandwidth.

Experiments have been performed[13] to verify the relationship between $\Delta\mu$ and a, i.e., $\Delta\mu = 1/S \approx \sqrt{a}$, and the relationship between $\Delta\mu$ and the amount of energy required to produce a detectable image. The relationship $\Delta\mu \approx \sqrt{a}$ was confirmed over a wide range of image areas (presumably over the range of areas for which $\sigma_a(\bar{D}) \approx 1/\sqrt{a}$) and the "minimum detectable energy" was determined to be 4 to 5 times $\Delta\mu$, where $\Delta\mu$ is computed at the optimum pre-exposure for a circular area having a diameter of 15 microns (see sub-section 2.2).

Other figures of merit have been evolved to characterize the detection properties of photographic emulsions, and detectors in general. Although these do not add to the basic theory, they have some usefulness for various special purposes, such as comparing different detectors or describing the degree of perfection achieved by a given detector. Some have received wide usage and, most importantly, published data is available in their terms.

"Incremental detectivity"[10], η, where

$$\eta = \frac{(aM)^{1/2}}{\Delta\mu} \tag{10}$$

η is the ratio of the energy an ideal detector requires for detection (assuming $\sigma(aM) \simeq \sqrt{aM}$) and that required by an actual detector.

"Detective quantum efficiency"[14], Q or $\hat{Q}$, where

$$Q = \hat{Q} = \eta^2 = \frac{aM}{\Delta\mu^2} = \frac{(S/N)^2_{\text{ideal}}}{(S/N)^2_{\text{measured}}} \tag{11}$$

This definition, where η is squared, makes Q equal to the "responsive" quantum efficiency of simple detectors such as the photoelectron tube where Q ≡ average number of observable events/incident photon.
S/N ≡ signal-to-noise ratio.

These relationships (Equation 3, 4, 10, and 11) must be used with care. They are derived basically by describing the random functions of noise and signal in terms of their standard deviation, σ. The distributions of the random functions are not specified so that the significance of σ in terms of the detection performance, or quality, is not apparent. (These matters are discussed in greater detail in sub-section 2.2.) An example of the need for caution is illustrated in Fig. 2[10], which shows that an emulsion having a higher maximum detective quantum efficiency, Q, is not necessarily the best detector.

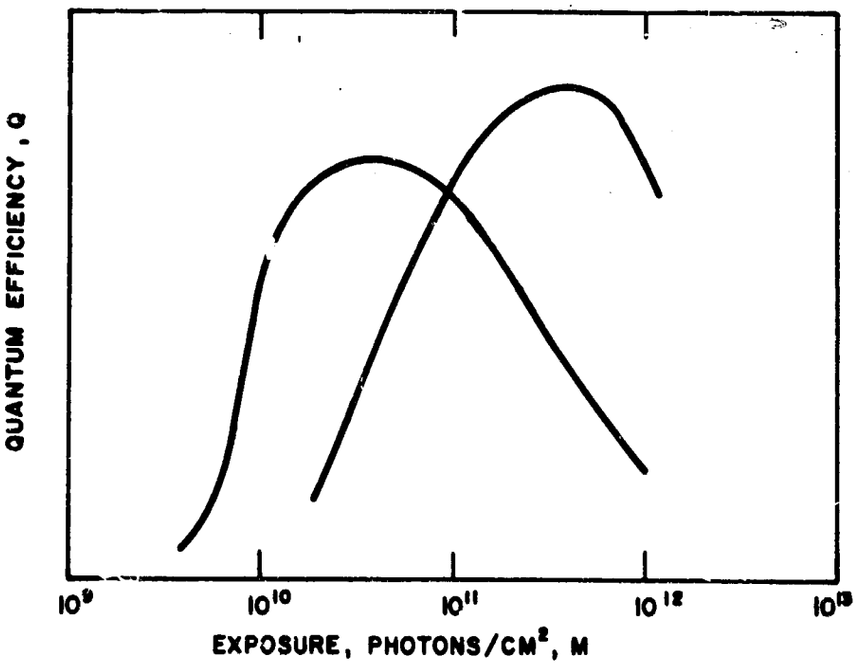

Fig. 2. Detective quantum efficiency of two emulsions.

Another point is brought up here because, when it is overlooked, erroneous estimates of the energy requirements for photographic detection can be made. Equations 3 and 5 indicate that the least detectable energy, $(a\,\Delta M^*)$, is proportional to the square root of image area (and scanning area), $\sqrt{a}$, over the range of areas that are of interest here. It is sometimes assumed that the energy required for a detectable density change over an area a is proportional to a, not to $\sqrt{a}$. This assumption is valid only when a is so large that $\sigma_a(\bar{D})$ is negligibly small in comparison with $\bar{D}$ and the statistical nature of D can be ignored.

2.2 THRESHOLD DETECTION OF STELLAR IMAGES

Detection is defined here as an observable event due to a signal, or a combination of signal and noise, which can be distinguished from observable events due to noise alone. The signal and irreducible noise are assumed to be random variables and detection is characterized in terms of the probabilities that an event due to noise alone can be mistakenly assumed to be a signal, P(fa), and that an event due to signal and noise will be so recognized, P(d). A detectable signal, in this sense, is one of sufficient magnitude so that P(fa) is acceptably small and P(d) is acceptably close to unity. In addition, these probabilities must apply over an interrogation area, A, where A is generally >> a, within which the location of the signal is in doubt.

The mathematical model for this description of detection is illustrated in Figs. 3 and 4. It is reasonable to assume that density due to noise and signal has a Gaussian distribution[3f][4d] (see also sub-section 3.3) in the range of image and scanning areas of particular interest.

Referring to Fig. 3,

$$D_T = \bar{D}_n + k_1 \sigma_a(\bar{D}_n) \tag{12}$$

and

$$\bar{D}_{s+n} - k_2 \sigma_a(\bar{D}_{s+n}) = D_T \tag{13}$$

$\bar{D}_n$ is the average emulsion density due to noise; $\sigma_a(\bar{D}_n)$ is the standard deviation of $\bar{D}_n$ over a scanning area, a; $\bar{D}_{s+n}$ and $\sigma_a(\bar{D}_{s+n})$ are similar parameters for signal and noise. D_T is the "threshold" value of density, that is, $D_n(x, y)$ has the probability P(fa) of being equal to or larger than D_T and $D_{s+n}(x, y)$ must be such that its probability of being $\geq D_T$† is P(d). P(fa) and P(d) are chosen standards of detection for a particular application. k_1 and k_2 are parameters such that P(fa) and P(d) have

† Note that D_T is an independent parameter whose value depends on the choice of $\bar{D}_n$ and P(fa).

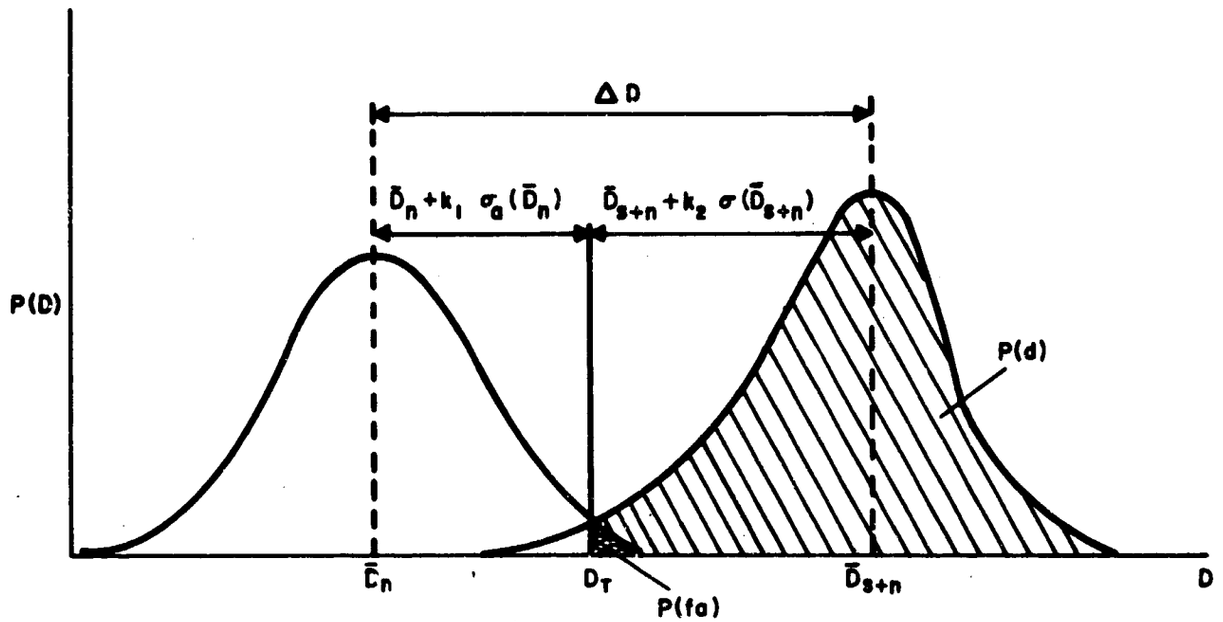

Fig. 3. Statistical model of photographic detection.

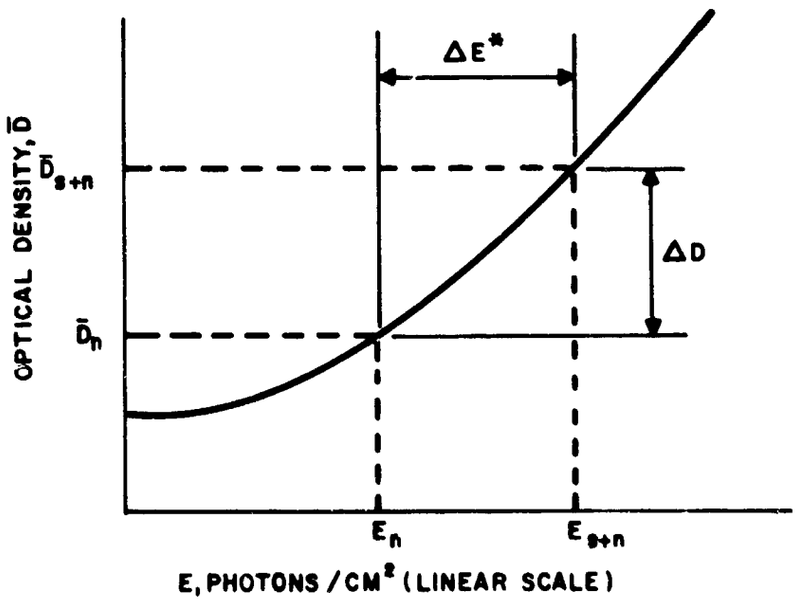

Fig. 4. Graphical illustration of ΔE^*, the minimum detectable energy.

approximately the desired values; they are readily found by reference to normalized Gaussian distribution tables.

Combining Equations 12 and 13,

$$\bar{D}_{s+n} = \bar{D}_n + k_1 \sigma_a (\bar{D}_n) + k_2 \sigma_a (\bar{D}_{s+a}) \qquad (14)$$

Figure 4 shows how the minimum exposure required for detection, ΔE^*, is determined from the measured characteristic function of the emulsion, when the values of $\bar{D}_n$ and $\bar{D}_{s+n}$ have been found. (E is used as a symbol for exposure rather than M in order to avoid confusion with previous relationships such as Equations 3 and 4.)

When the operating point ($\bar{D}_n$, E_n) can be chosen, the procedure for finding ΔE^* for a given emulsion is as follows:

a. Find the characteristic function of the emulsion ($\bar{D}$, E) over the range $\bar{D}$ of interest, by measurement or from published data.

b. Find the standard deviation of $\bar{D}$, $\sigma_a (\bar{D})$, over the range of $\bar{D}$ of interest. The scanning area, a, will be approximately the area of the stellar camera's circle of confusion.† It may be convenient to use the relationship that

$$\sigma_a (\bar{D}) \approx \frac{1}{\sqrt{a}}$$

c. Using Equation 4, where $g = \overline{\Delta D} / \Delta E$, find the value of E where S is a maximum; this value will be the operating, or pre-exposure, point (E_n, $\bar{D}_n$, $\sigma_a (\bar{D}_n)$).

d. Find k_1, using a table of areas under the standard normal curve,†† from the relationship

$$\frac{A}{a} \left[0.5 - A_S (k_1) \right] \approx P(fa), \qquad P(fa) << 1 \qquad (15)$$

† For near threshold images on the PC-1000 Stellar Camera this is an approximately circular area about 60 microns in diameter.

†† For example, Handbook of Chemistry and Physics, 46th Edition, Chemical Rubber Co., Cleveland, Ohio, 1965-1966, pp. A114-A116.

A is the interrogated area on the photographic plate, A_S is the area under the standard normal curve as the Gaussian parameter, k_1 †, increases from 0.

e Compute D_T from Equation 12.

f. Find k_2, with the same table used for finding k_1, where

$$\left[0.5 + A_S(k_2)\right] = P(d) \tag{16}$$

g. Compute $\bar{D}_{s+n}$ from Equation 14. An exact solution of Equation 14 requires a successive approximation. For some emulsions (sub-section 2.3),

$$\sigma_a(\bar{D}_n) \simeq \sigma(\bar{D}_{s+n}) \tag{17}$$

so that

$$\bar{D}_{s+n} \simeq \bar{D}_n + (k_1 + k_2)\,\sigma_a(\bar{D}_n) \tag{18}$$

is a reasonable approximation.

h. Find E_n, E_{s+n} and then $\Delta E^* = E_{s+n} - E_n$ from the characteristic curve of the emulsion. The minimum energy required for detection is then $a\Delta E^*$ photons.

2.3 EVALUATION OF SPECTROSCOPIC EMULSION, KODAK TYPE 103-F

Type 103-F is one of the red-sensitive spectroscopic emulsions that has been widely used for geodetic satellite photography in projects ANNA, GEOS, and LARGOS. At this time we know of no other emulsions that are available on glass plates which have been demonstrated to be superior for the purpose.

---

† Or t in the notation of the referenced table, footnote † † on preceding page.

Figure 5 is a plot of the measured characteristic function of this emulsion. Exposures for obtaining this curve were made over a spectral bandwidth of about 15Å centered at 6940Å. Exposure times varied from 0.05 to 1.1 seconds as the average developed density varied from 0.16 to 1.0.† The methods used to take this data, and other data referred to in this section, are discussed in Section 3. Figure 6 is a plot of the measured standard deviation of $\bar{D}$ for emulsion 103-F as a function of $\bar{D}$: $\sigma_a(\bar{D})$ (solid line) was computed from data obtained with a microdensitometer aperture of 480 microns^2. The dashed curve in Fig. 6 is for a scanning area of 1950 microns^2 (50-micron diameter), and is obtained from the relationship

$$\sigma_a(\bar{D}) \approx \frac{1}{\sqrt{a}} \quad \text{(sub-sections 2.2 and 3.3)}$$

Figure 7 is a plot of the emulsion sensitivity, S, of 103-F emulsion in accordance with Equation 4 and the data in Fig. 5 and 6. The peak sensitivity is near a pre-exposure density of 0.3, so that 0.3 (2.5×10^{10} photons/cm^2 exposure) is assumed to be the optimum operating point.

Let the acceptable detection quality parameters be

$$P(fa) = 10^{-2}$$

$$P(d) = 0.98$$

and the interrogated area, A, be 27.8×10^4 microns^2,†† and the scanning area, a, be 1950 microns^2.

Then, from Equations 15 and 16 (also referring to tables of normal distribution curve areas),

$$k_1 = 3.7$$

and

$$k_2 = 2.0$$

---

† A test was made (sub-section 3.3) to determine the extent of reciprocity-law failure at threshold of detection exposure levels over an exposure time range of 4 to 100 milliseconds; there is no evidence of a significant failure of the reciprocity law in these measurements.

†† This implies an uncertainty of about 2 arc-minutes in the location of the image on the plate of the PC-1000 Stellar Camera, where 1-in. displacement at the focal plane $\equiv 1.4^o$.

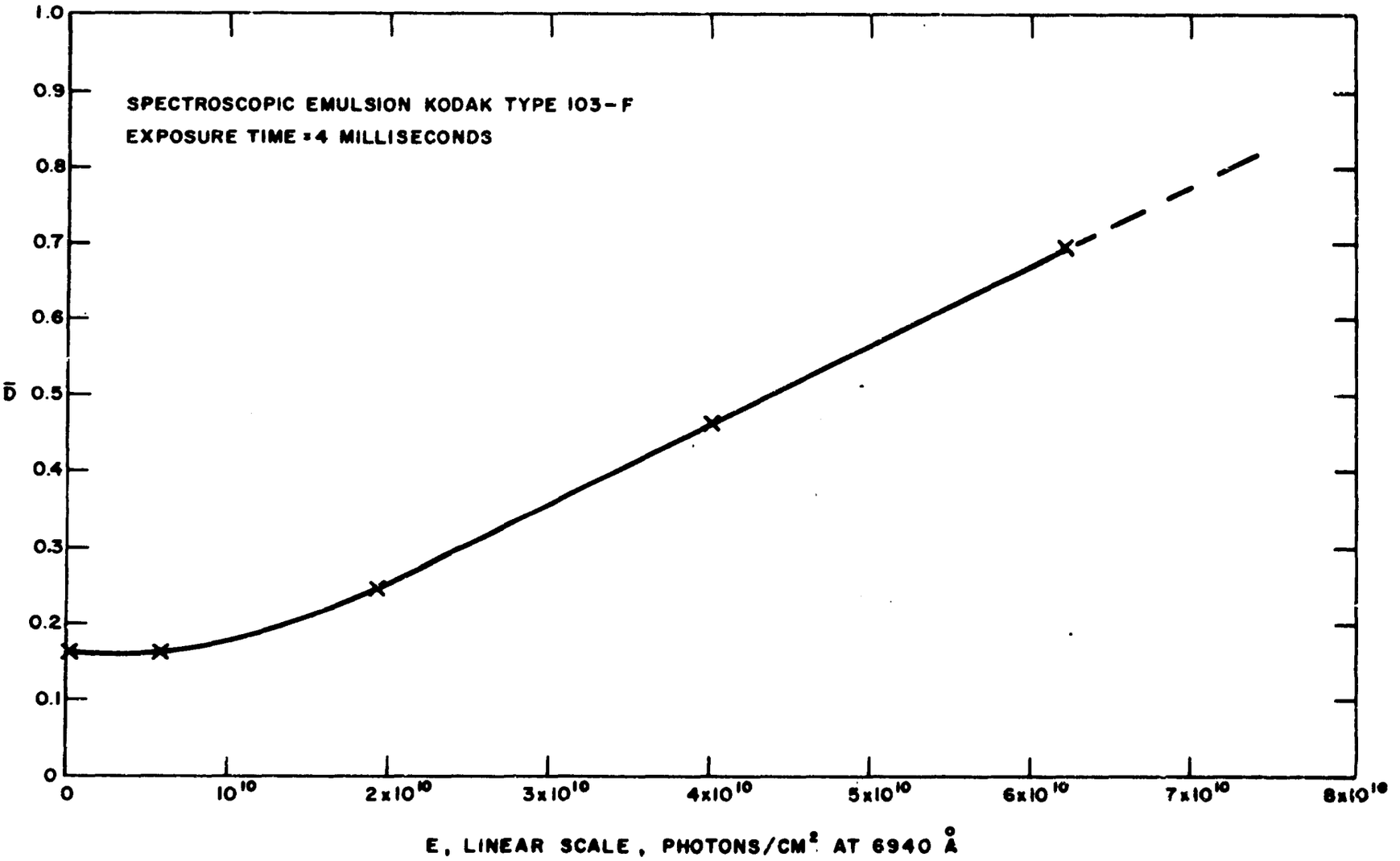

Fig. 5. Measured characteristic function of Kodak spectroscopic emulsion Type 103-F.

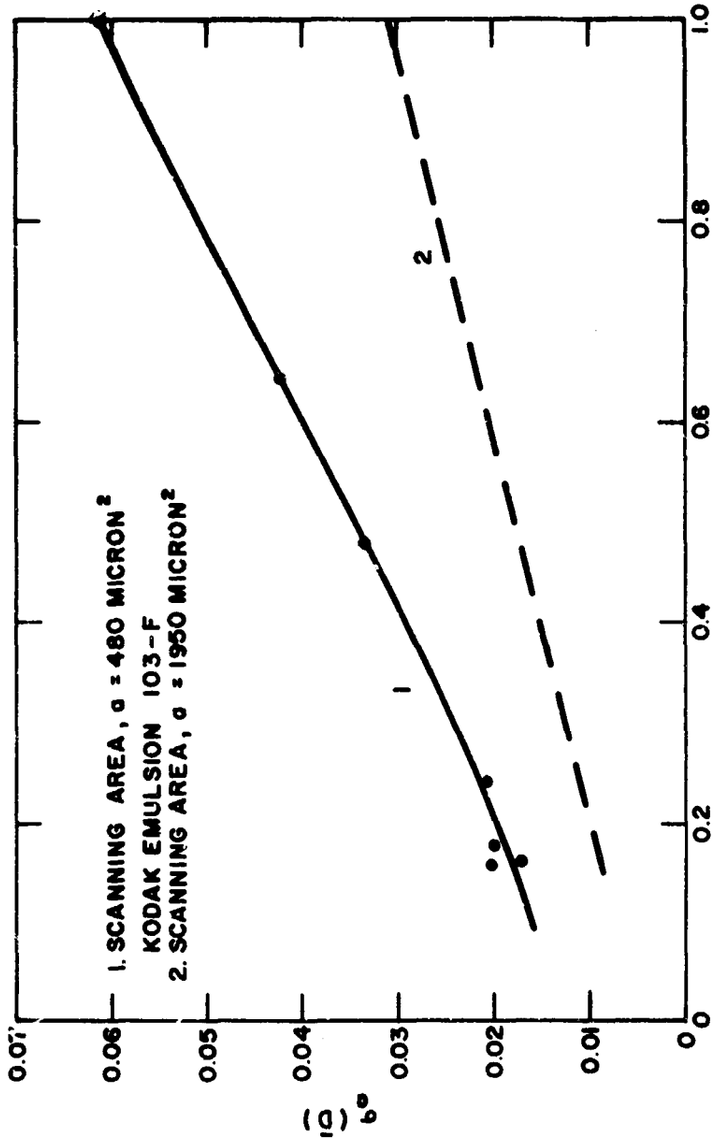

Fig. 6. $\sigma_a(\bar{D})$ vs $\bar{D}$ for emulsion Type 103-F.

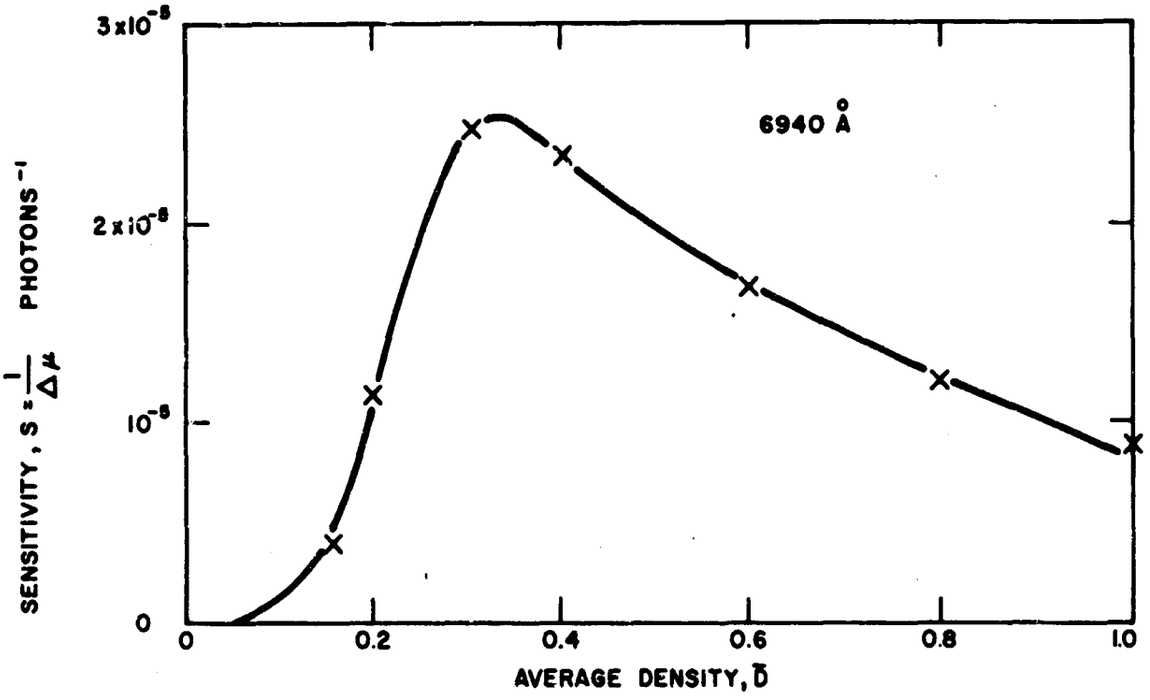

Fig. 7. Sensitivity vs average density for emulsion Type 103-F.

Solving for D_T in Equation 12,

$$D_T = 0.30 + 3.7\,(0.0125) = 0.347$$

Solving for $\bar{D}_{s+n}$ in Equation 13; assume as a trial that $\bar{D}_{s+n} = 0.38$, then $\sigma\,(\bar{D}_{s+n}) = 0.015$ and

$$0.38 - 2\,(0.015) = D_T = 0.350$$

This is close enough agreement, so that for detection of a 50-micron diameter spot in a 595-micron diameter field on 103-F emulsion,

$\bar{D}_n = 0.30$ (with pre-exposure)

$\bar{D}_{s+n} = 0.38$

$\Delta D = 0.08$

$\Delta E^* = 3.25 \times 10^{10} - 2.50 \times 10^{10} = 0.75 \times 10^{10}$ photons/cm^2 (from Fig. 5),

and the minimum energy required is

$$a\Delta E^* = 146,000 \text{ photons (at } 6940\text{Å})$$

Equations 12 and 13 will now be solved for the case where there is no pre-exposure and background illumination is assumed to be negligible. Then,

$$\bar{D}_n = 0.16$$
$$\bar{D}_T = 0.16 + 3.7\,(0.01) = 0.20$$

Assume

$$\bar{D}_{s+n} = 0.22; \text{ from Equation 13 and Fig. 6,}$$

$$D_T = 0.22 - 2\,(0.01) = 0.20$$

Then,

$$\Delta D = 0.06$$
$$\Delta E^* = 1.5 \times 10^{10} \text{ photons/cm}^2$$
$$a\Delta E^* = 295,000 \text{ photons}$$

About twice as much energy is required in this case for the same result, which demonstrates the value of pre-exposure, under these conditions, in order to obtain the maximum emulsion sensitivity. (See also Reference 15 for a discussion of the pre-exposure of spectroscopic emulsions.)

From Equations 6 and 8 and the experimentally measured values of $\sigma_a(\bar{D})$ vs $\bar{D}$, the value of α for emulsion 103-F is about $2.3\ \mu^2$ and $G \simeq 0.3/\mu^2$. The average grain count in an area of approximately 50-μ diameter is of the order of hundreds of grains so that detection by grain count is not practical. Furthermore, the formation of large clumps of grains at the densities of most interest would preclude an accurate grain count even for emulsions, such as Type 1-N, where G is much smaller.

It is interesting to compare the results of this analysis with those obtained from the subjective (visual) threshold detection experiment described in sub-section 3.3.2. In any experimental verification it must be kept in mind that the signal energy has been assumed in this analysis to be uniformly distributed over the image area and to have affected the average density over this entire area. This is a reasonable assumption

to make insofar as detecting the presence of the signal is concerned; the distribution of the signal energy and that of density in the image area must be considered insofar as the location of the image is concerned and these matters are discussed in sub-sections 2.5 and 3.3.4.

2.4 EFFECTS DUE TO CHARACTERISTICS OF LASER ILLUMINATION (COHERENCE AND INTERMITTENCY)

When a coherent optical plane wave is incident on an optically rough reflector, the resulting reflection pattern has numerous major lobes. If the receiver aperture intercepts only a part of one lobe and the response of the detector to a determinate signal is governed by Poisson statistics,† the detector response to statistically independent detection trials is then a random function with a Bose-Einstein distribution.†† The effect of such a distribution is generally to seriously reduce the probability of detection from that obtained if the target is optically smooth and the received energy is determinate; or conversely, much more energy must be transmitted for a correspondingly high detection probability. If numerous statistically independent detection trials are correlated, for example by (synchronous) integration of the received signal energy, the detector response is then described by a negative-binomial distribution; as the number of such correlated trials becomes large (say greater than 10), this distribution becomes a close approximation to the Poisson distribution, and the detection situation is the same, for practical purposes, as if the target were optically smooth.

In geodetic satellite photography, using a laser illuminator and an array of small cube corners for the reflector, the transmitted energy intercepted by the target will be highly coherent during the microsecond or less duration of each individual "spike" of the normal-mode laser output, and the target will be optically rough at the laser wavelength of about 6935Å. Thus, the response to received energy from each output spike is expected to obey Bose-Einstein statistics. However, a high-energy laser illuminator having an output of hundreds of joules will generally lase in the normal mode for at least 2 milliseconds and in this period will have of the order of 10^3 output spikes. The signal energy received from all these individual output pulses is correlated by virtue of the integrating properties of the photographic emulsion and the

---

† For example, a phototube[16] or a photographic emulsion (sub-section 2.1).

†† [16] and the references therein.

(practically) fixed spacial position of the unresolved satellite image during the lasing period. The overall effect is therefore expected to be the same as if the target were specular and the received energy determinate.

The laser spiking phenomenon also results in an intermittent exposure.(3g)(4e)(17) Webb (17) demonstrated that the effect of intermittent exposure is related to reciprocity-law failure, and that if the frequency of the intermittent energy pulses is sufficiently high, for a given average exposure intensity, the effect on the emulsion is the same as if it were exposed, over the same period of time, to a constant intensity having a value equal to the average intensity of the intermittent pulses. The frequency of the output pulses from a ruby laser operating in the normal mode is very high, approximately 200 kHz, and the peak intensity on the emulsion is expected to be very low, about of the order of 2×10^7 photons/cm^2 (6×10^{-5} ergs/cm^2 at 6935Å); i.e., approximately 500 pulses with an average of 2×10^7 photons/cm^2/pulse for a total of 10^{10} photons/cm^2. We therefore conclude that the intermittency effect will be the same as that due to failure of the reciprocity law for a low-level exposure over a period of between 2 and 3 milliseconds (sub-section 3.3).

It should be noted that the effect of atmospheric turbulence on the received signal has been neglected and that this may have a significant effect on the statistics of photographic detection.

2.5 LOCATION OF THE STELLAR IMAGE

The intrinsic lower limit on the accuracy with which a stellar object can be located photographically has been analyzed(18). The basis of this analysis is that the grain density distribution of an unsaturated image, $G_1(x, y)$, and hence the density, has a Gaussian shape in the vicinity of the peak values to a first order approximation. The assumptions and results may be qualitatively explained in the following manner. The incident radiation from the stellar object at the image plane can generally be expected to have a distribution near its peak intensity approximating the bell-shaped Gaussian function; the response of the photographic emulsion is statistical so that the distribution of the signal intensity, as determined by that of the image density, is distorted,† and so the location of the peak signal intensity is subject to some irreducible statistical error.

† This distortion is illustrated in the microdensitometer plots of threshold images in Fig. 19.

If the image is circularly symmetrical and is not saturated (in a photographic sense),† then the lower bound on the rms error in locating it is [using Farrell's notation(18)] .

$$B_x^{-1} = \frac{\sigma_x}{\left[N_s I_o(r)\right]^{1/2}} \quad \text{microns} \tag{19}$$

where σ_x is the Gaussian-shape parameter along the x coordinate; because of symmetry, $\sigma_y = \sigma_x$.

σ_x is found from the measured density profile of the image by fitting this profile to the Gaussian distribution curve shape at the peak and "one-sigma" points, as illustrated in the sketch labeled as Fig. 8.

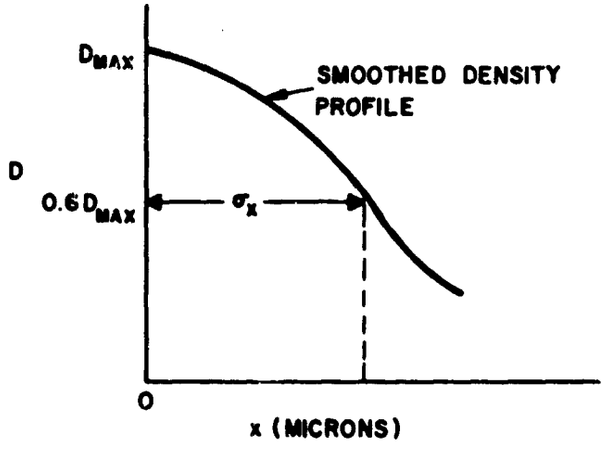

Fig. 8. Determination of σ_x from image density profile.

$N_s \equiv$ mean number of grains produced by the stellar object = $2\pi \sigma_x^2 G_1 (0, 0)$.

† The assumptions of symmetry and nonsaturation are reasonable for threshold and near-threshold exposures of short duration, so that ellipticity of the image should be small. It should be emphasized that threshold image symmetry pertains only to smoothed, or averaged, density profiles.

$I_o(r)$, $> 0 < 1$, is a function of the signal-to-noise ratio, r, plotted in Fig. 9, and

$$r = \frac{N_s}{\pi \sigma_x^2 G_b} = \frac{2 G_1 (0, 0)}{G_b} \qquad (20)$$

G_1 (0, 0) is the grain density (mean number of grains/unit area) at the center of the image due to signal alone and G_b is the grain density of the background. Grain density, G, is approximately related to emulsion density, D, and transmission, T, as follows:

$$G = \frac{1}{0.434 \alpha} D = \frac{1}{\alpha} \ln \frac{1}{T} \text{ grains/unit area}$$

where α is the area of the developed grain.

This analysis will be applied to get some idea of the penalty for threshold detection of signal presence in terms of location error. Threshold and above-threshold exposures of the same point source will be compared in this respect (sub-section 3. 2. 4).

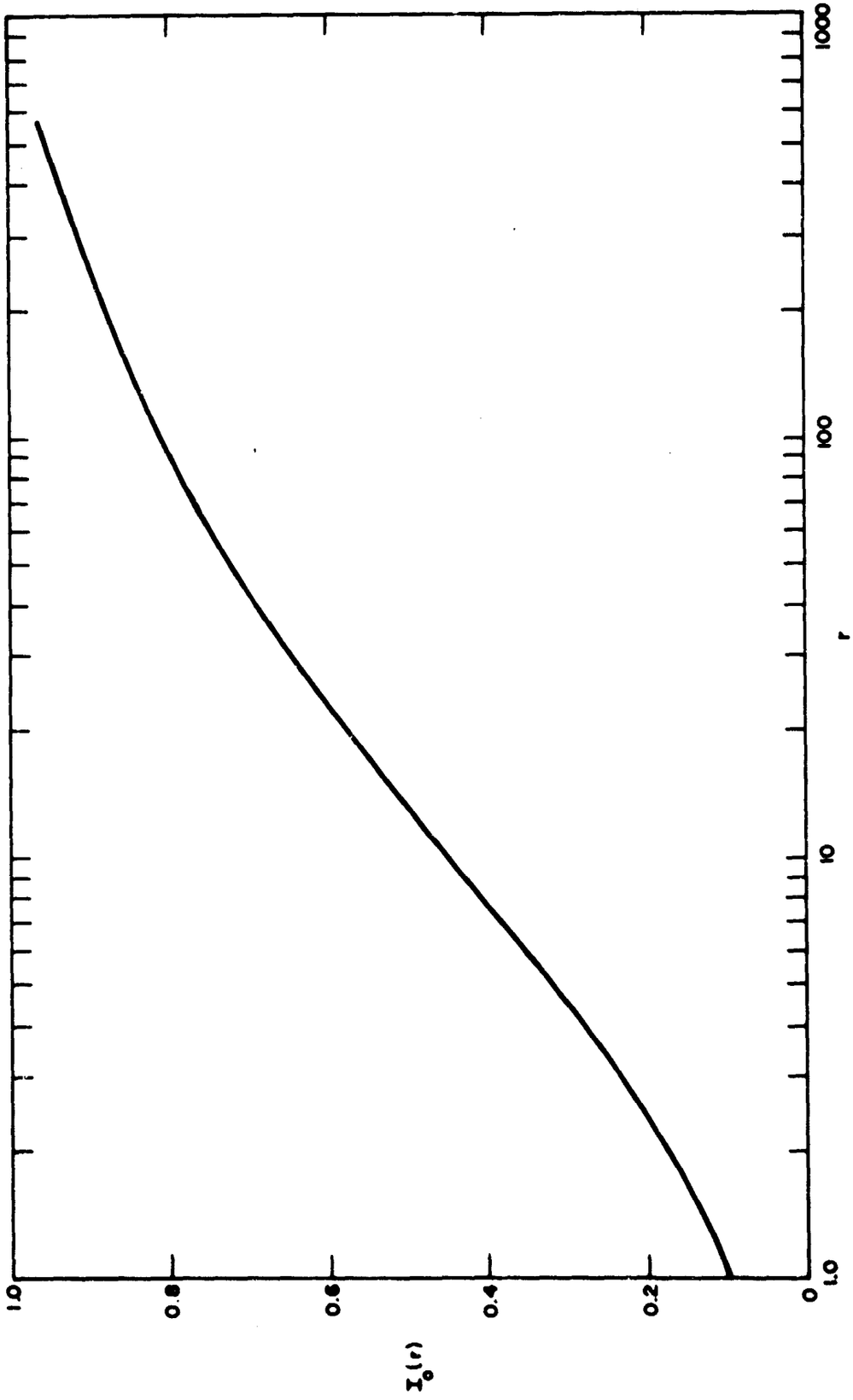

Fig. 9. $I_o(r)$ vs signal-to-noise ratio.

SECTION 3

EXPERIMENTAL STUDY

3.1 GENERAL

As pointed out in Section 2, the detection performance of a photographic emulsion must be determined largely on the basis of empirical measurements of its characteristic function and statistical properties. Specifically, these measurements should be made in such fashion that they reflect the conditions of a particular application, so that spectral response, reciprocity-law failure, and any other pertinent characteristics of the emulsion are taken into account. Since such data as these are not known to be available for the emulsions and the conditions of interest, the following experimental work was performed:

(1) Measurement of the characteristic function of spectroscopic emulsion KodakType 103-F at 6940Å.

(2) Measurement of the statistical properties of 103-F as a function of average density. A scanning aperture area is used so that the standard deviation of the density, $\sigma_a(\bar{D})$, is inversely proportional to $\sqrt{a}$.

(3) Measurement of the threshold energy at 6940Å required to obtain a "just-detectable" image of about 50-microns diameter by visual examination. Spectroscopic emulsions Types 103-F, 1-N, and 103a-U (all red-sensitive) were used in these tests. These results are to be compared to the results obtained in Section 2 for emulsion 103-F.

(4) Determination of exposure reciprocity over an exposure-time range of from 4 to 100 milliseconds.

(5) Smoothed density profiles of threshold and above-threshold images are obtained to compare estimated intrinsic location errors.

3.2 EXPERIMENTAL EQUIPMENT AND METHODS

Figure 10 is an illustration of the experimental setup used to obtain data for determining the characteristic function of an emulsion. The photomultiplier sensitivity in amp/watt at 6940Å was previously

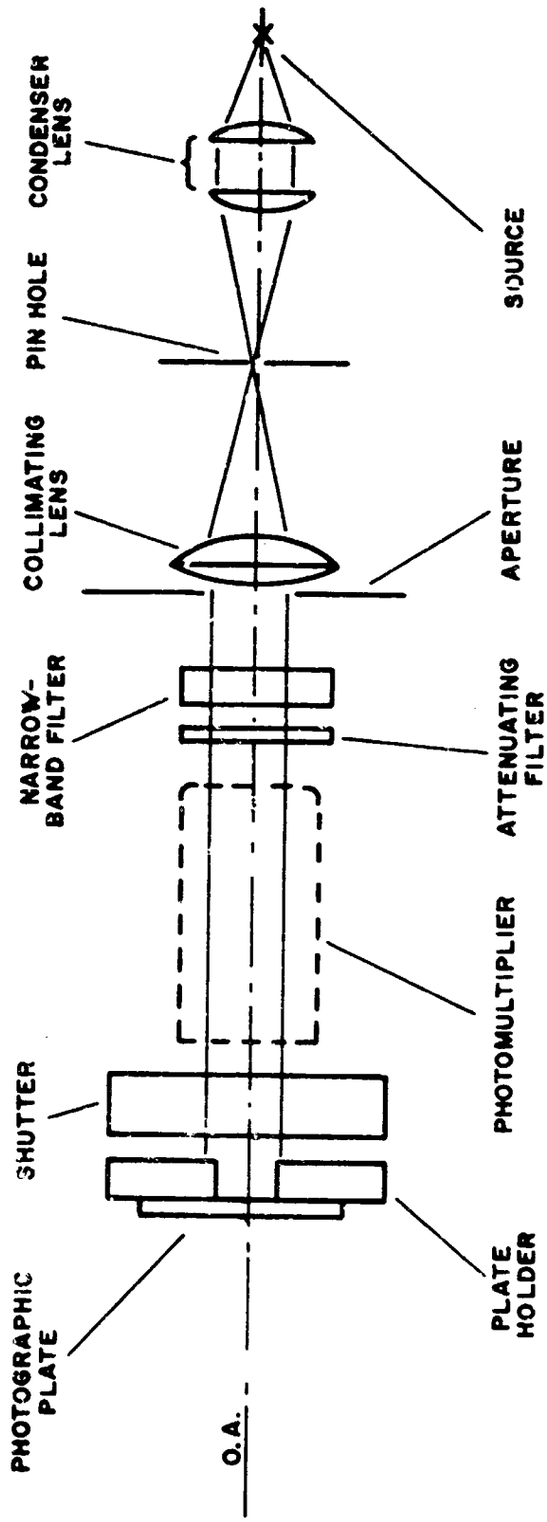

Fig. 10. Experimental setup for characteristic function data.

measured† and the shutter speeds calibrated. The stability of the photomultiplier detector, that of the shutter operation, and that of the source lamp were frequently checked; it is believed that exposure was measured to better than 20% throughout the experiments described in this section. Measurement system parameters and relationships used are summarized below:

Photomultiplier:	EMI Type 9558B
Narrow-band filter:	Peak wavelength – 6940Å Spectral pass band – 20Å Peak transmission – 45% Sideband transmission – < 0.1%
Photomultiplier calibration:	3.7×10^{3} amp/watt at 6940Å and 1000V on dynodes.
Photomultiplier dark current:	3.6×10^{-9} amp with 1000V on dynodes.

1 photon ≡ 2.87×10^{-19} watt-sec at 6940Å

$$\text{No. of photons} = \frac{I_{pm}\,\tau}{S_{pm}} \left(\frac{10^{19}}{2.87} \right)$$

where I_{pm} = photomultiplier current in amp, S_{pm} = photomultiplier sensitivity in amp/watt at 6940Å and with same dynode voltage, τ is the exposure time in seconds, and the wavelength of the radiation is 6940Å.

Pinhole diameter:	12 microns
Exposed area on plate:	0.142 in.^2 (0.425 in. dia)
Beam diameter from collimator:	0.500 in. (1.27 cm)

† The photomultiplier was calibrated by means of the spectral irradiance from a plane tungsten emitter of known area and temperature. The same narrow-band interference filter was used in this calibration as was used subsequently in the test setups of Figs. 10 and 11.

Collimator lens:	Achromat, F. L. = 190 mm, Dia = 55 mm
Calibrated shutter speeds used:	0.05, 0.17, 0.60, and 1.12 sec
Source:	75-watt, high-pressure xenon arc lamp

Micro-density measurements of exposed areas were made with a recording microdensitometer by the Photo Image Analysis Dept. of Itek Corp. in Lexington, Mass.

Figure 11 shows the optical bench setup used to obtain small images of from 25 to 50-microns diameter. These are essentially diffraction-limited spots, the sizes of which were measured by a calibrated microscope. The purpose here was to simulate the energy distribution of a stellar image more closely than would be possible with a pinhole mask. The shutter was adjusted for an exposure of 4 milliseconds when making threshold energy tests† and was varied over a calibrated range of from 4 to 100 milliseconds during the tests for reciprocity-law failure at threshold levels. Parameters for this setup are the same as previously described with the following exceptions:

Pinhole diameter:	6 microns
Focusing lens:	Achromat, F. L. = 190 mm, Dia = 55 mm

Significant change in the optical path between the source and the emulsion plane was avoided after focus and spot size were checked with the microscope. Thin gelatin attenuating filters were used to this end although ordinarily these are not as desirable as glass filters.

Microphotographs at magnifications 100X and 450X were made at EG&G; microphotographs at a magnification of 257X were made at Itek Corp.

† This is as close to the 2.5-millisecond laser period as was possible with the mechanical shutter available.

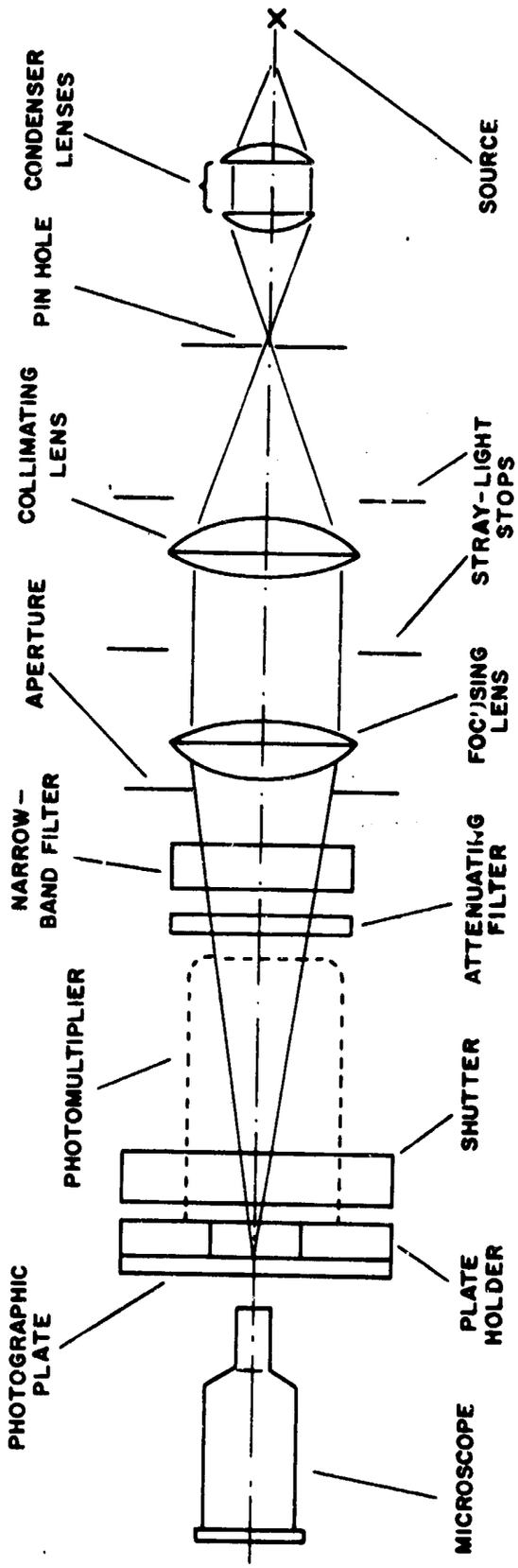

Fig. 11. Experimental setup for threshold energy tests.

3.3 EXPERIMENTAL MEASUREMENTS

3.3.1 Characteristic Function and Statistical Data on Emulsion Type 103-F

Figure 12 shows reproductions of samples from microdensitometer traces of developed 103-F emulsion. The test conditions and the results of interest are summarized in Table 1. $\bar{D}$ and $\sigma(\bar{D})$ were computed from the following relationships:

$$\bar{D} = \frac{\sum_{i=1}^{N} D_i}{N} \tag{21}$$

and

$$\sigma(\bar{D}) = \left[\frac{\sum_{i=1}^{N} D_i^2}{N} - \bar{D}^2 \right]^{1/2} \tag{22}$$

D_i are statistically independent values of D taken from plots like those shown in Fig. 12, and N is the total number of such samples used. N = 80 for the results shown in Table 1. A sample calculation of Plate No. 3 is shown in the Appendix to this report.

Figure 13 is a series of 275X microphotographs of 103-F emulsion Plate No. 3, 4, 6, and 7. These photographs illustrate the difficulty of using actual grain count instead of density† as a measure of photographic response to exposure; note that the formation of large clumps of grains at average densities of interest (> 0.2) make a reasonably accurate counting of developed grains difficult, if not impossible.

† or grain density, derived from optical density, Equation 6.

Table 1. Summary of experimental data on emulsion Type 103-F.

Plate No.	Exp. (photons/cm^2)	$\bar{D}$(†)	$\sigma(\bar{D})$(††)	Exposure Time (seconds)
2	0	0.16	0.017	0
3	0.16×10^{10}	0.16	0.019	0.05
4	0.54×10^{10}	0.17	0.020	0.17
5	1.9×10^{10}	0.25	0.021	0.60
6	3.8×10^{10}	0.47	0.033	1.12
14	6.0×10^{10}	0.64	0.042	1.12
7	10.9×10^{10}	1.01	0.061	1.12

(†)Development procedure: Developed for 4 minutes in D-19 (full strength) at 68°F with constant agitations. Fixed for 5 minutes at 68°F with constant agitations. Washed for 10 minutes.

(††)Scanning aperture: 8 x 60μ ($480\,\mu^2$). Number of sampled points used to calculate $\sigma(\bar{D})$ = 80.

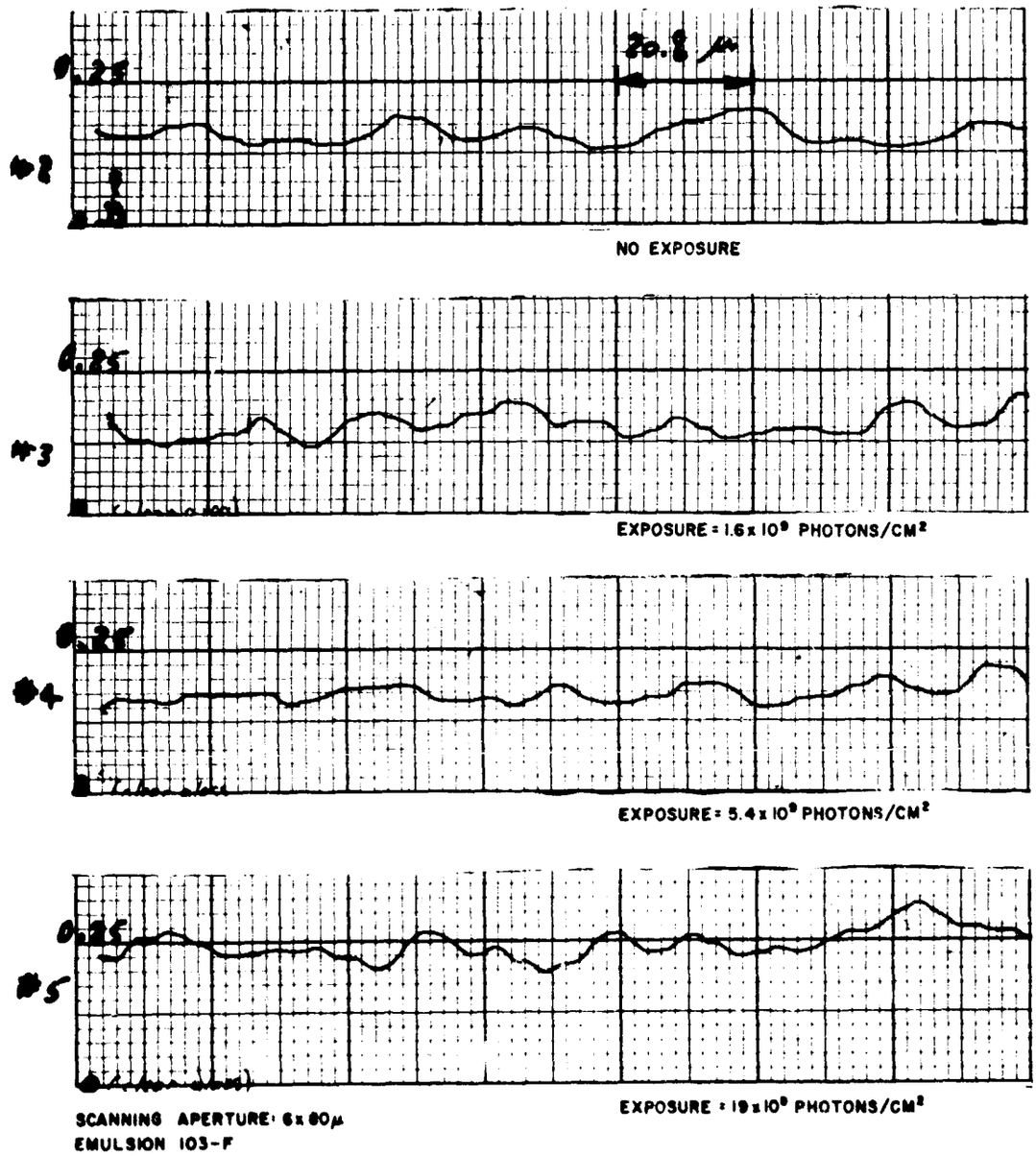

Fig. 12. Samples of microdensitometer data for characteristic function and statistical characteristics (sheet 1 of 2).

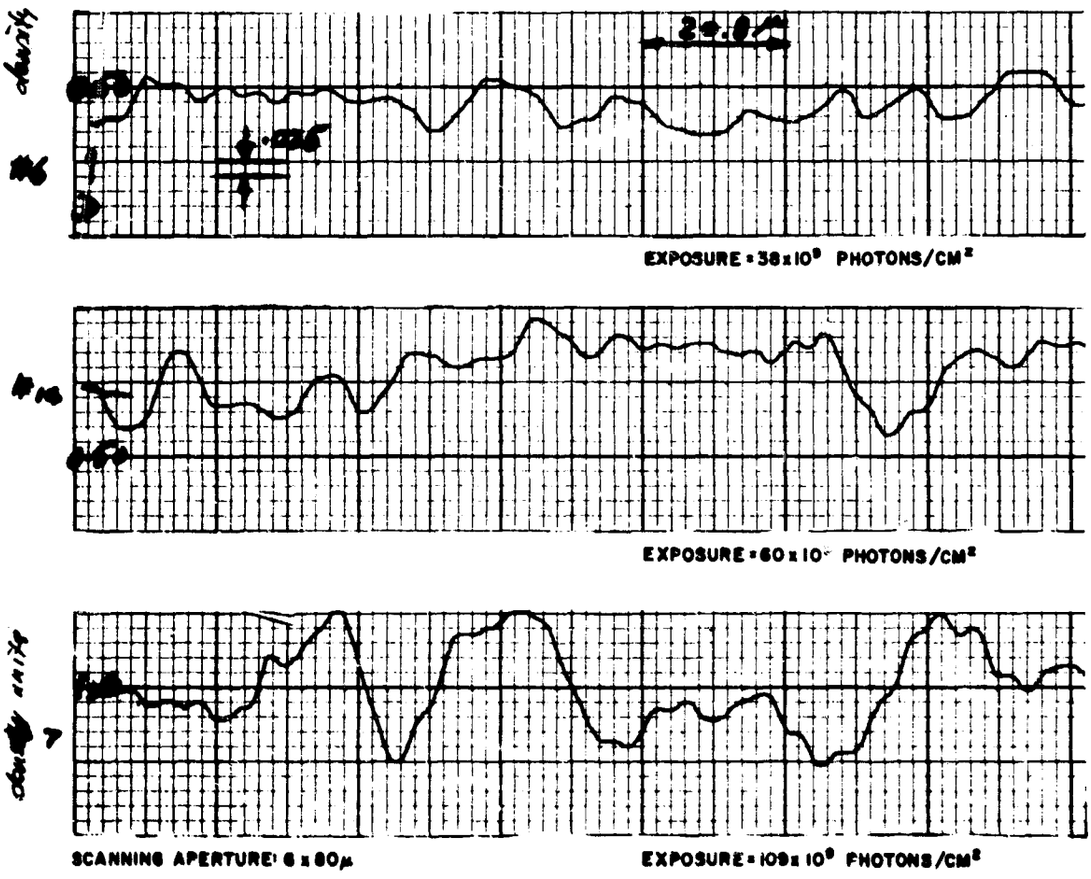

Fig. 12. Samples of microdensitometer data for characteristic function and statistical characteristics (sheet 2 of 2).

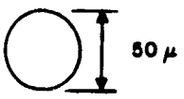

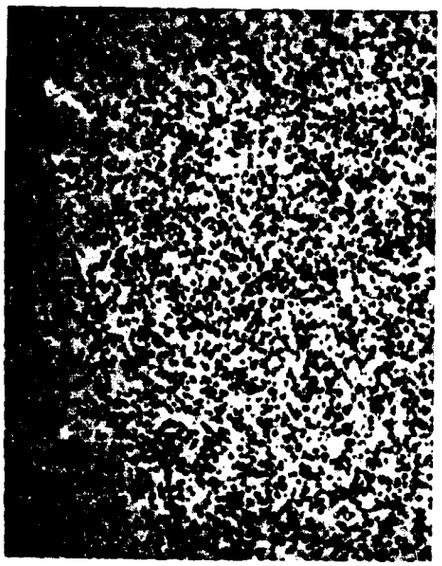

PLATE NO. 3 $\bar{D}$ =0.16

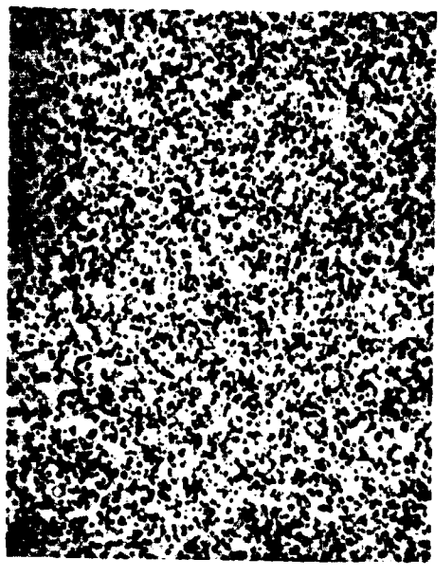

PLATE NO. 4 $\bar{D}$ = 0.17

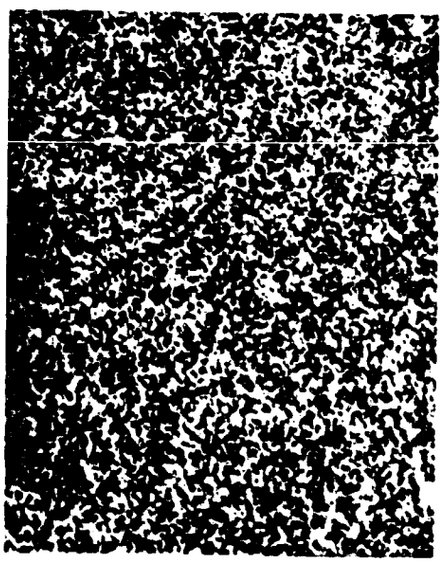

PLATE NO 6 $\bar{D}$ = 0.47

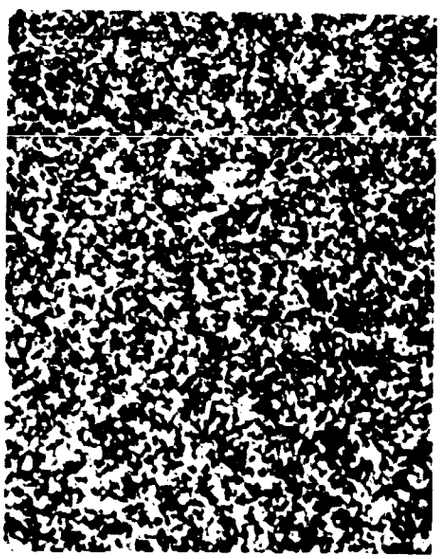

PLATE NO. 7 $\bar{D}$ = 1.01

MAGNIFICATION: 274 X

Fig 13 Microphotographs of Plate No. 3, 4, 6, and 7 (Fig. 12).

A test was made of the statistical distribution of densities using the data obtained with the microdensitometer on developed plates having average densities of 0.16, 0.25, and 0.64. The results are plotted in Fig. 14 and show that the assumption of a normal distribution is a good one, at least out to about $\pm$ 2.2 σ. The limited number of samples (80) precludes a good evaluation beyond these points.

3.3.2 Threshold Energy Measurements

"Threshold" images were produced by progressively reducing exposure, using the setup described in sub-section 3.2 and illustrated in Fig. 11. In this case the "threshold" is defined in a subjective sense, that is, as the minimum stellar image whose presence could be visually detected with some degree of confidence by an observer aided by optical magnification of from 100X to 450X. In this context detection does not have the meaning described in Section 2; although these images are subjectively detectable, there is no quantitative measure of assurance that they are not due to noise. In these experiments the locations of the images are known so that confusion with noise is very unlikely; that there could otherwise be such confusion is demonstrated by microphotographs of signal-and-noise images in Figs. 15-17, and of images due to noise alone in Fig. 18.

Figures 15-17 show a number of (subjectively) threshold images on spectroscopic emulsions Types 103-F, 1-N, and 103a-U. As indicated, the exposure time for all these images is 4 milliseconds, the illumination is nearly monochromatic at 6940 Å, and the images are essentially those of a diffraction circle approximately 50 microns in diameter with a signal energy of approximately 4.5×10^5 photons. No pre-exposure was used in any of these tests. A few initial things of particular interest about the results of these experiments are noted:

(1) If the signal energy is reduced by a factor of 2, the images are definitely not detectable by visual examination, at any magnification, and even when the observer knows exactly where the image is located on the plate.

(2) The images shown in Figs. 15-17 are virtually impossible to find without substantial magnification, of about 100X and greater. One important reason for this is that dirt, pits, and other emulsion imperfections cannot be distinguished at lower magnifications.

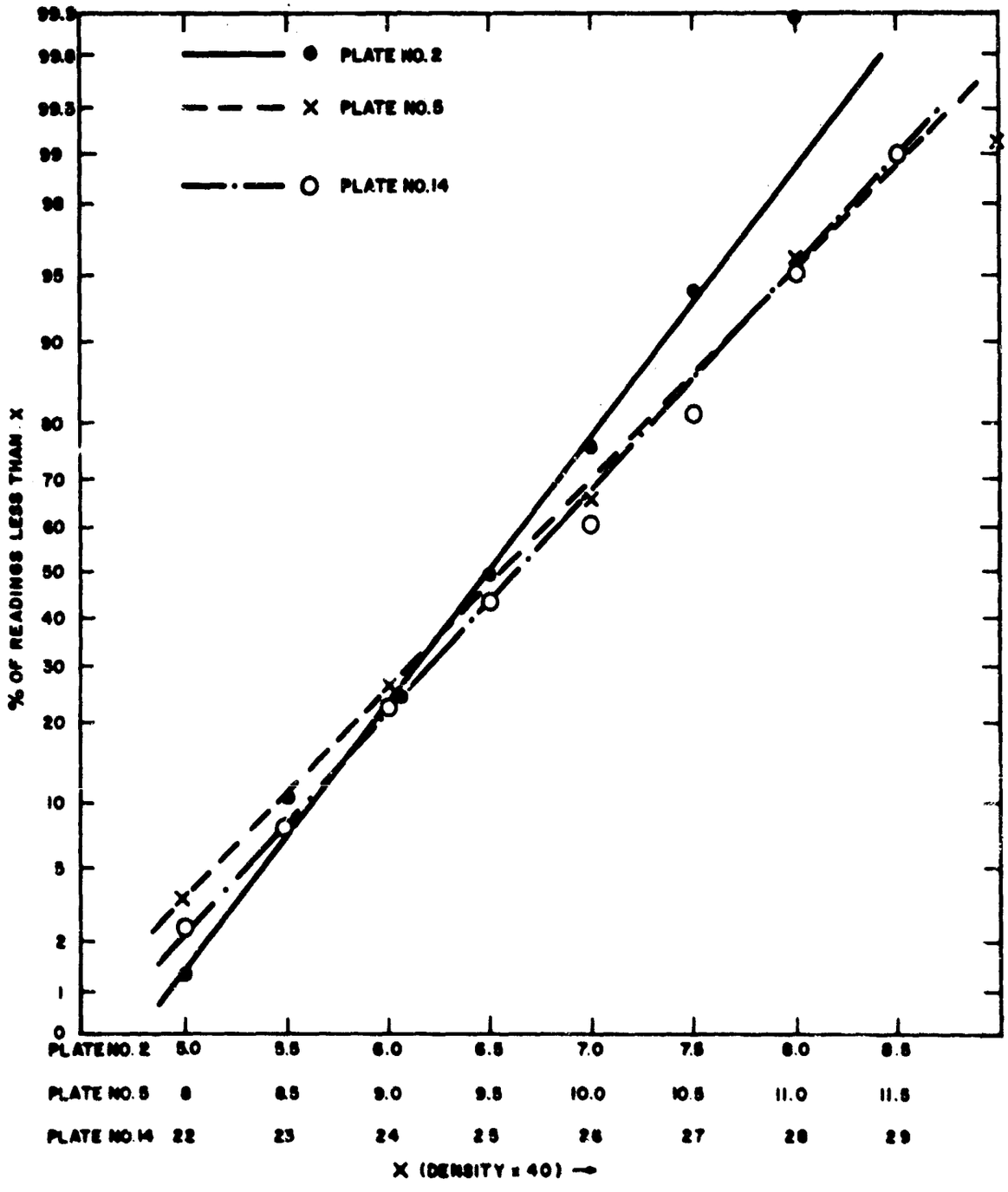

Fig. 14. Tests for normal distribution of density in Type 103-F emulsion samples.

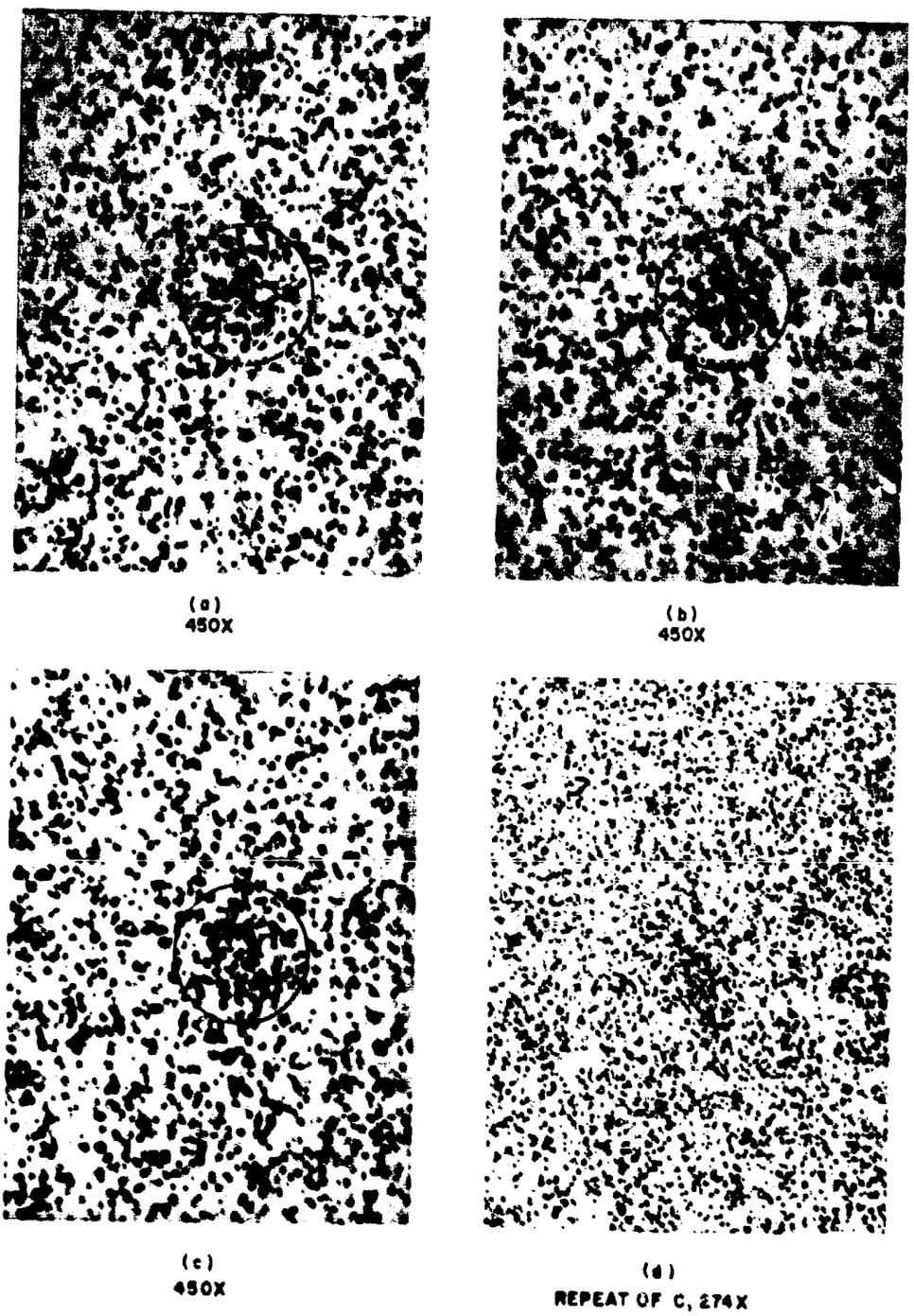

Fig. 15. Microphotographs of threshold stellar images on Type 103-F emulsion.

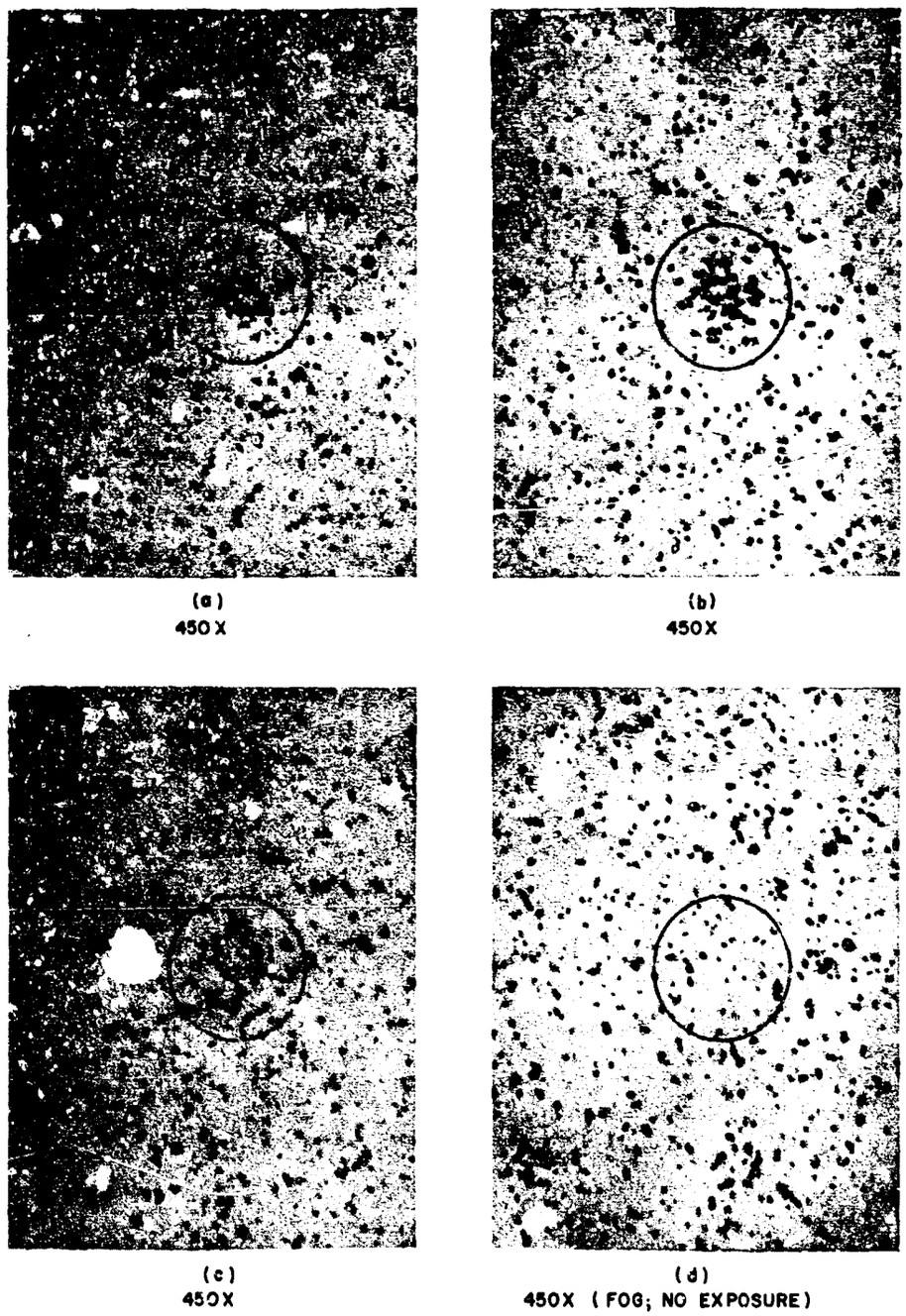

ALL EXPOSURES TAKEN ON SAME PLATE; EXPOSURE TIME = 4 MILLISEC; APPROX ENERGY IN CENTER DIFFRACTION CIRCLE OF 50-μ DIA = 4.5×10^6 PHOTONS AT 6940 Å (NO PRE-EXPOSURE). RECTICLE CIRCLE DIA = 50 μ.

Fig. 16. Microphotographs of threshold stellar images on Type 1-N emulsion.

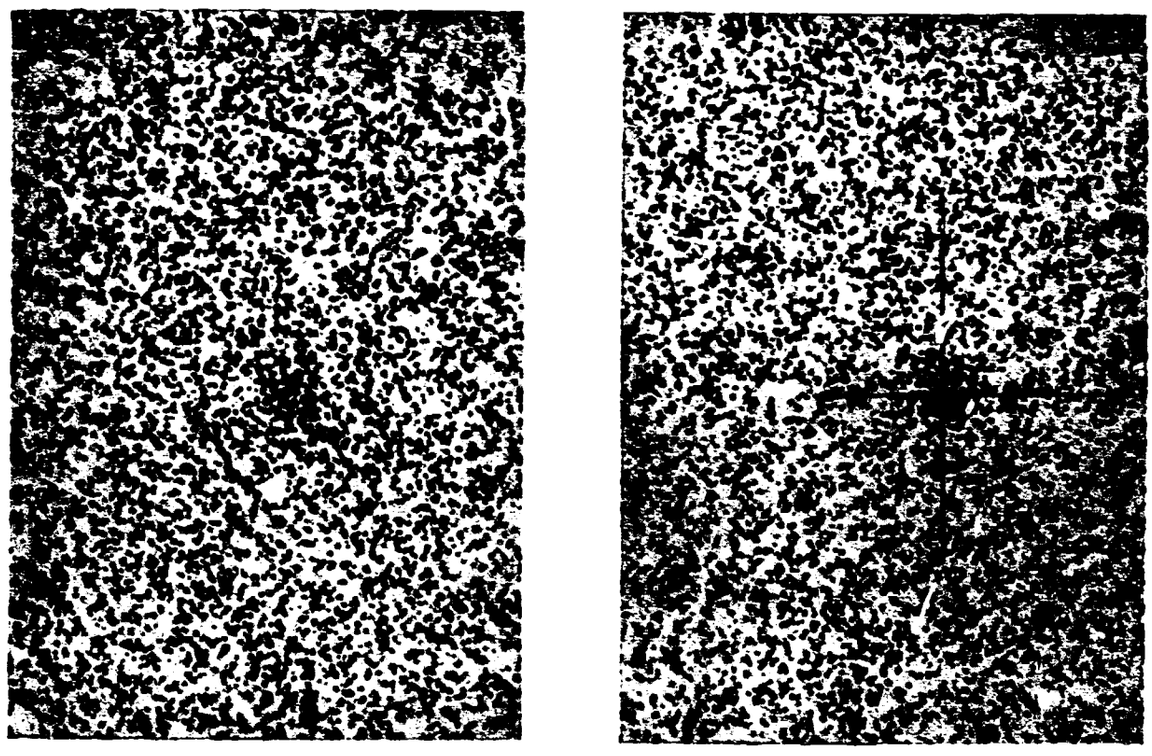

(a)
274X

(b)
274X

EXPOSURES TAKEN ON SAME PLATE; EXPOSURE TIME = 4 MILLISEC; APPROX ENERGY IN CENTER DIFFRACTION CIRCLE OF 50-μ DIA = 4.5×10^6 PHOTONS AT 6940 Å (NO PRE-EXPOSURE).

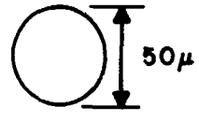

Fig. 17. Microphotographs of threshold stellar images on Type 103a-U emulsion.

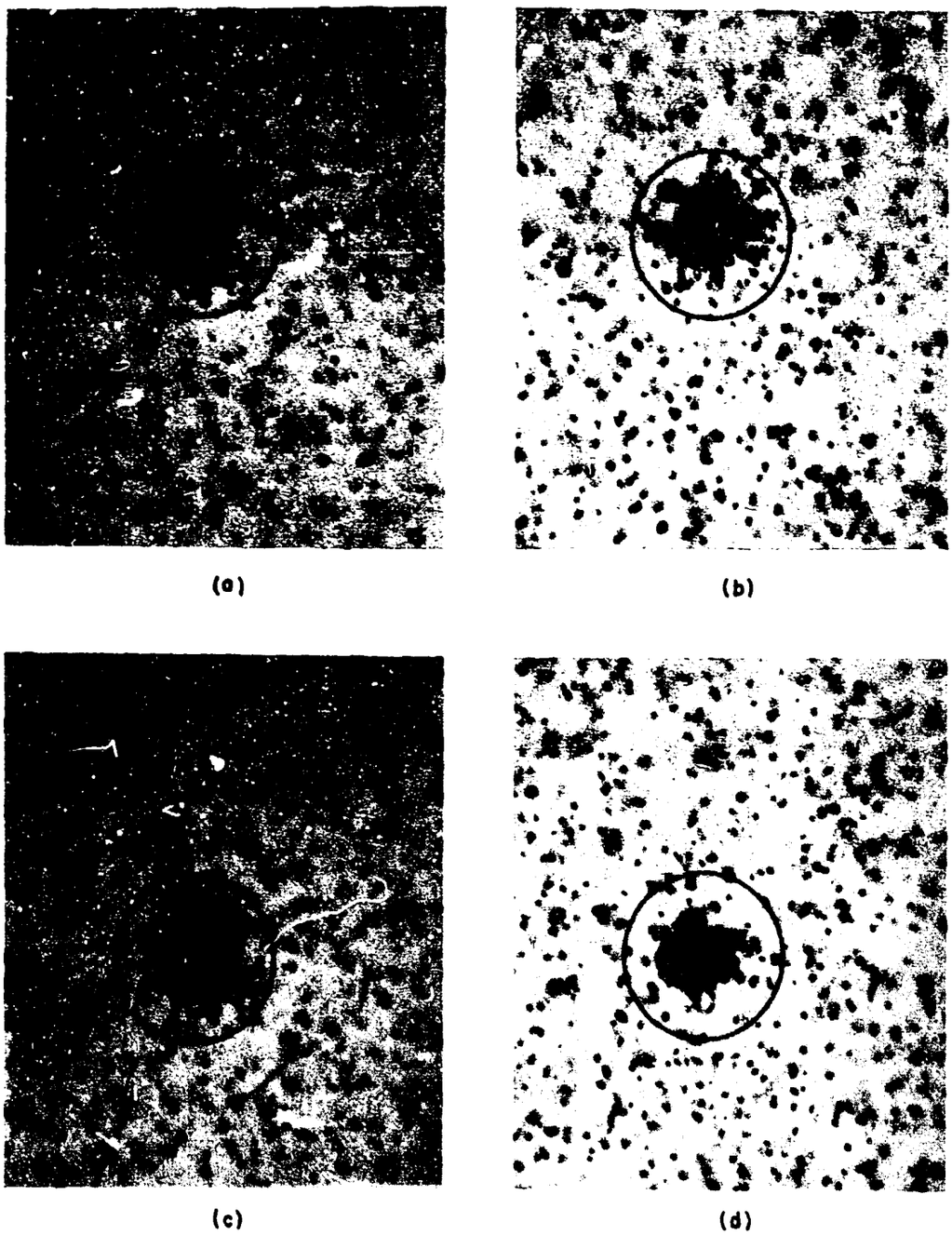

Fig. 18. Microphotographs of images due to noise.

(3) Figures 15-17 reveal the statistical nature of the photographic process qualitatively.

(4) The energy required for subjective threshold detection is closely the same for spectroscopic emulsions Types 103-F, 1-N, and 103a-U, although these emulsions have different fog levels and statistical characteristics. The required energy is somewhat higher than predicted in sub-section 2.3 for objective detection with 103-F emulsion, 4.5×10^5 photons vs 3×10^5 photons.

(5) The experimental threshold images have a significantly higher peak density (averaged over a 50-μ diameter) and signal-to-noise ratio than is predicted to be necessary for objective detection (see Fig. 19). The average for a number of such images on 103-F emulsion is as follows:

$$\bar{D}_{s+n} \text{ (experimental)} = 0.30$$

$$\bar{D}_{n} \text{ (experimental)} = 0.14$$

$$S/N \text{ (experimental)} = \frac{\bar{D}_{s+n} - \bar{D}_{n}}{\bar{D}_{n}} = 1.1$$

For the same non pre-exposure case, the predicted detection requirements are (sub-section 2.3)

$$S/N = \frac{0.22 - 0.16}{0.16} = 0.37$$

Some of the foregoing difference could be due to the inexact nature of subjective detection. There has not been sufficient experimental work in this area to come to a firm conclusion but it is quite possible that visual detection is significantly less sensitive than instrumental detection because the human observer is poor at analyzing the random pattern of grains representing a photographic signal embedded in noise.

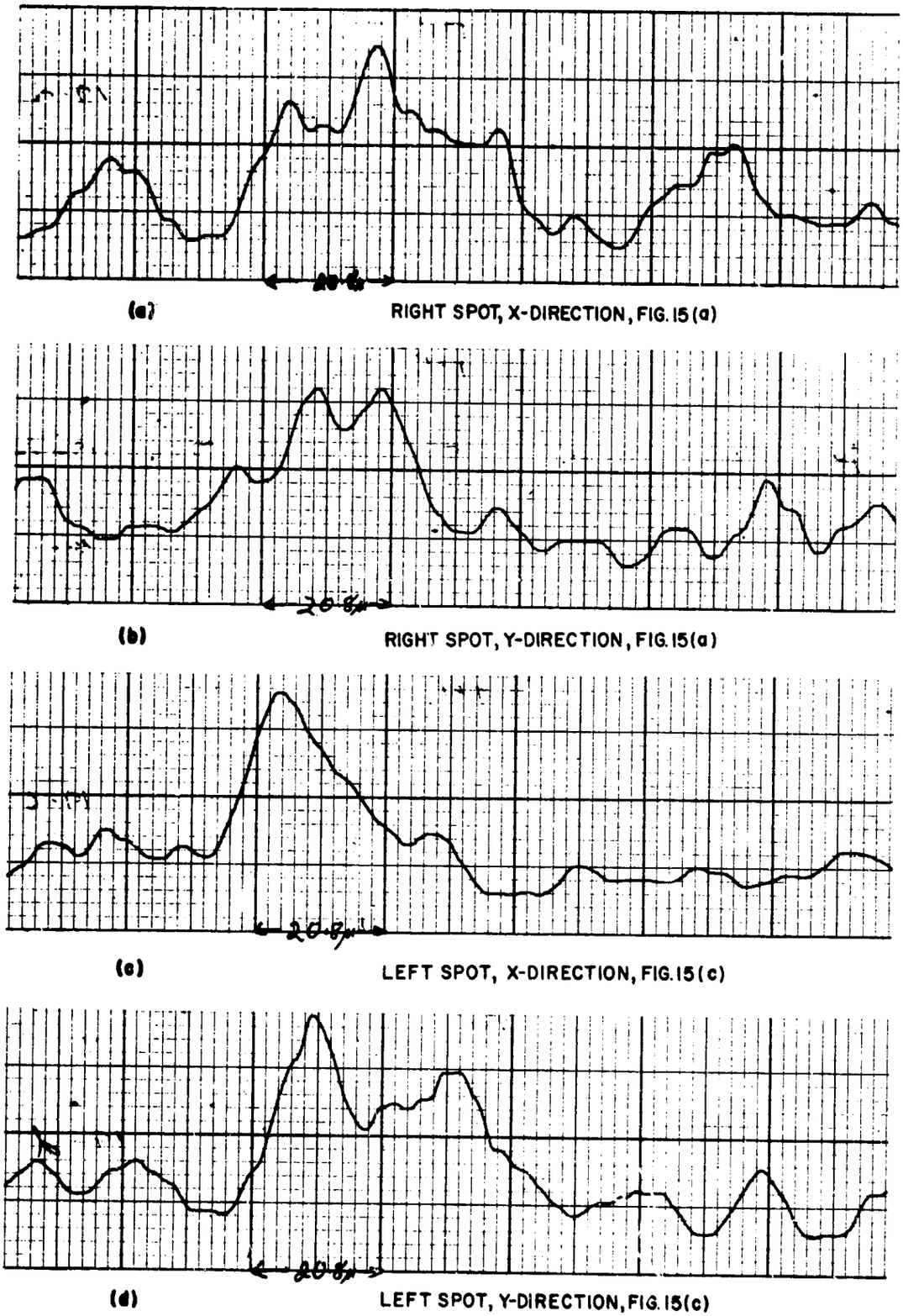

Fig. 19. Microdensitometer plots of threshold stellar images (sheet 1 of 2).

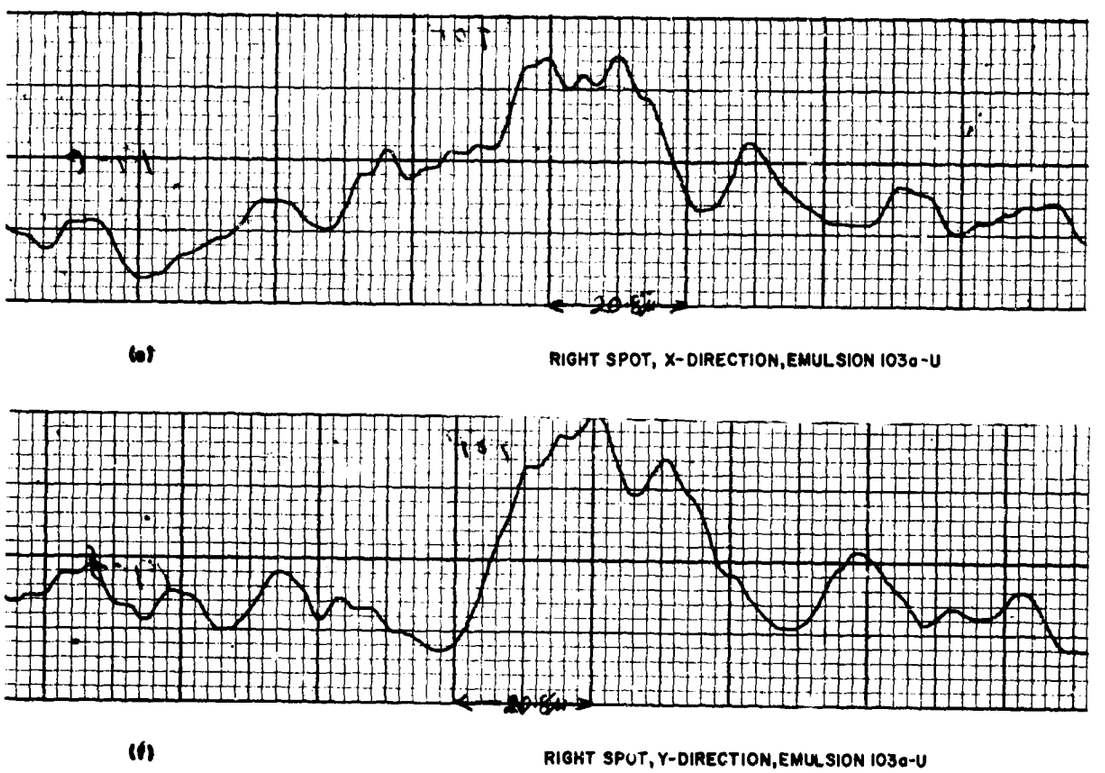

Fig. 19. Microdensitometer plots of threshold stellar images (sheet 2 of 2).

3.3.3 Exposure Reciprocity Measurements

Experiments were conducted to determine failure of the reciprocity law for exposure times from 4 to 100 milliseconds; the available mechanical shutter was not capable of accurately controlling exposure time outside of this range.

The technique used is to compare stellar images obtained with the same total energy over the available range of exposure times. The energy used was about 4.5×10^5 photons, i.e., the energy previously determined to be required for subjective threshold detection. The results are illustrated in Figs. 20 and 21. There is no evidence of significant reciprocity-law failure in these emulsions under the conditions of the experiments. The expected exposure time for laser illumination of geodetic satellites is approximately 2.5 milliseconds. Photographic emulsions, in general, exhibit little, if any, reciprocity-law failure from 0.1 to 1 second. It is therefore believed that the data for determining the characteristic function of 103-F (Table 1) is valid for the conditions of interest herein.

3.3.4 Measurement of Intrinsic Image Location Error

Two images on emulsion 103-F, one close to threshold and one well exposed, are to be compared with respect to intrinsic image location error. Microphotographs of these images are shown in Fig. 22, their microdensity plots appear in Fig. 23, and their "smoothed" density profiles are given in Fig. 24. Minimum rms location error will be computed for these widely different exposures in accordance with the analysis in reference (18).

- For the near-threshold image,

$\bar{D}_n$ (average background density) = 0.14

α (grain area) = $2.3\ \mu^2$

D_s (peak signal density) = 0.37 - 0.14 = 0.23 (Fig. 24)

σ_x = 27 μ (Fig. 24)

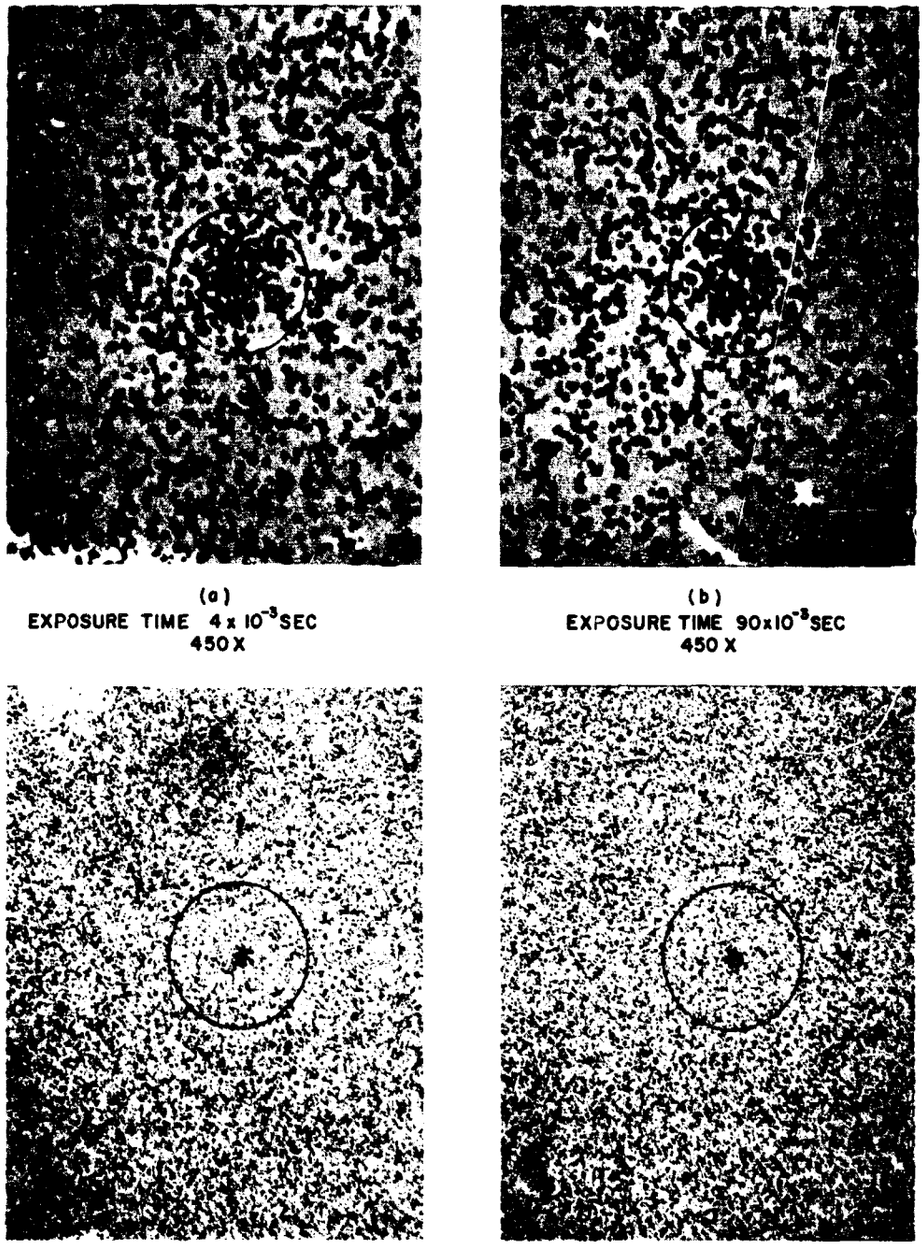

TOTAL ENERGY IN BOTH EXPOSURES APPROX ≈4.5 x 10^5 PHOTONS AT 6940 Å WITHIN 50-μ DIA CIRCLE (NO PRE-EXPOSURE).

Fig. 20. Microphotographs of exposure reciprocity tests on Type 103-F emulsion.

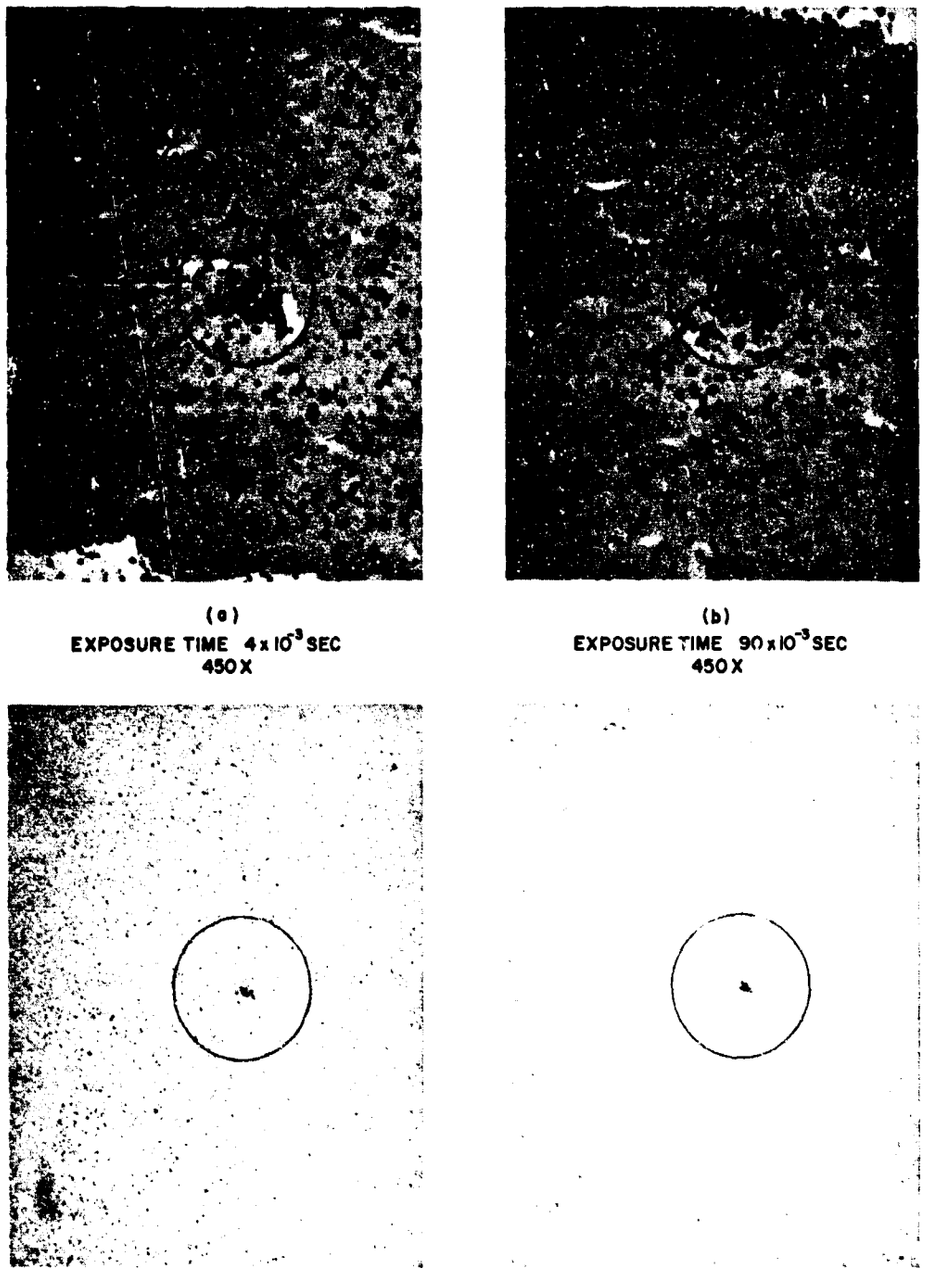

Fig. 21. Microphotographs of exposure reciprocity tests on Type 1-N emulsion.

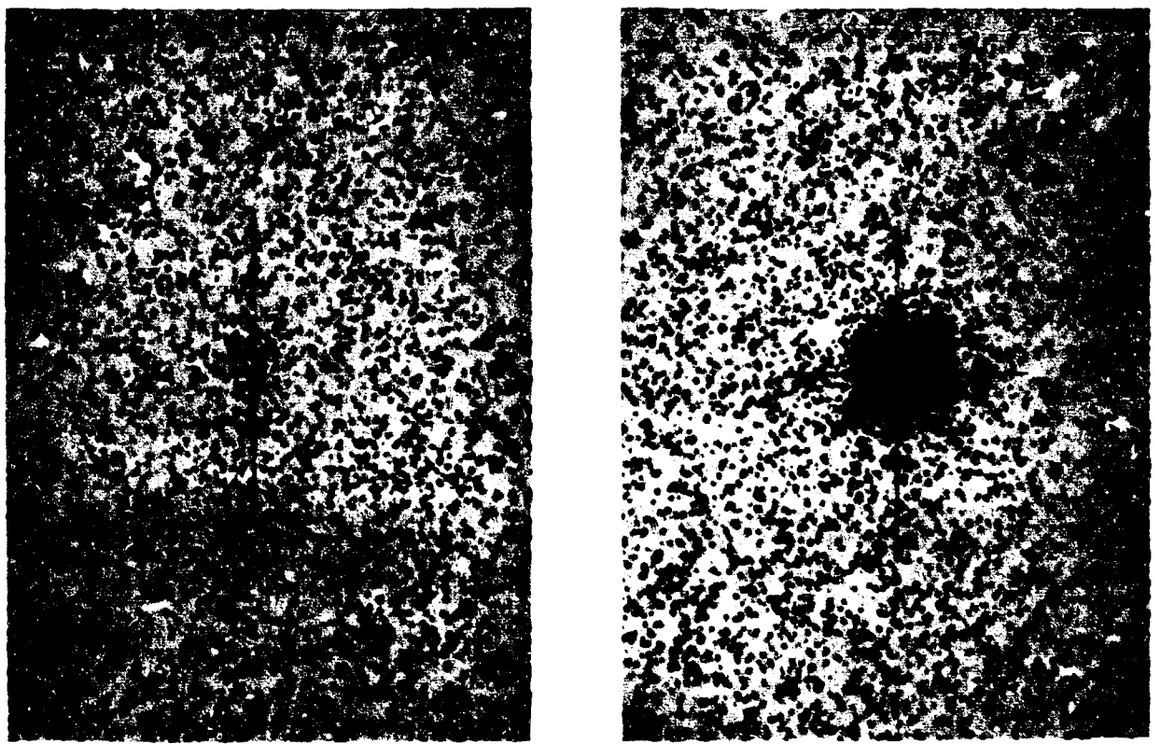

(a)
NEAR-THRESHOLD IMAGE

(b)
WELL-EXPOSED IMAGE

MAGNIFICATION 274X
TYPE OF EMULSION 103-F

Fig. 22. Microphotographs of images used for comparison of minimum rms location error.

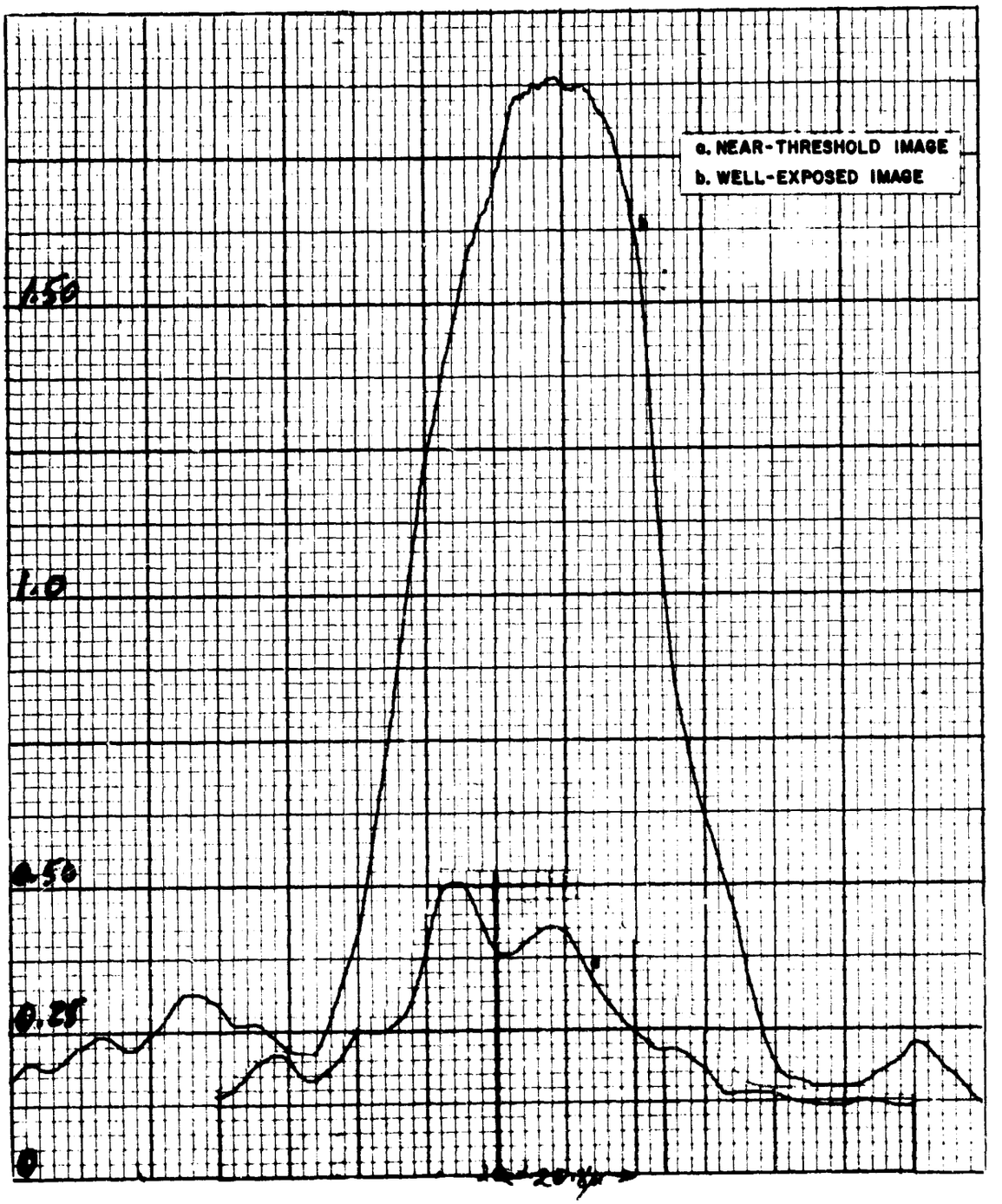

Fig. 23. Microdensitometer plots of images in Fig. 22.

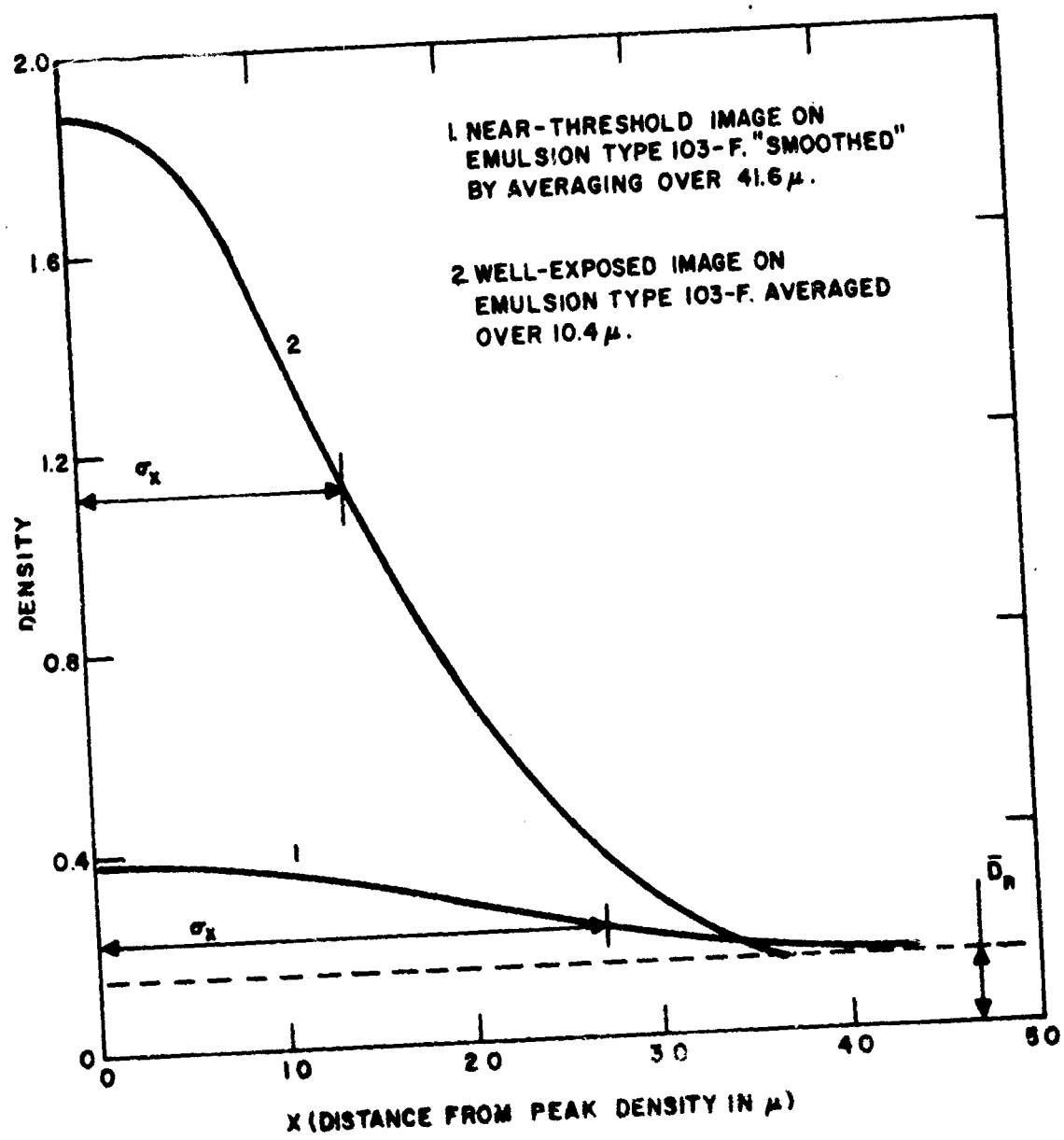

Fig. 24. Density profiles of near-threshold and well-exposed images on emulsion Type 103-F (Fig. 22 and 23).

Then,

$$G_b = \frac{\bar{D}_n}{0.434\alpha} = 0.14 \text{ grain}/\mu^2 \qquad \text{(Equation 8)}$$

$$G_1(0, 0) = \frac{D_s}{0.434\alpha} = 0.23$$

$$r \text{ (signal-to-noise ratio)} = \frac{2G_1(0, 0)}{G_b} = 3.3$$

$$I_o(r) = 0.22 \quad \text{(Fig. 9)}$$

N_s (no. of exposed grains due to signal) =

$$2\pi\sigma_x^2 G_1(0, 0) = 1,050$$

$$\text{Min. rms location error} = \frac{\sigma_x}{\left[N_s I_o(r)\right]^{1/2}} = 1.8\,\mu$$

For the well-exposed image,

$\bar{D}_n = 0.14$

$\alpha = 2.3\,\mu^2$

$D_s = 1.88 - 0.14 = 1.74$ (Fig. 24)

$\sigma_x = 15\,\mu$ (Fig. 24)

and

$G_b = 0.14 \text{ grain}/\mu^2$

$G_1(0, 0) = 1.74$

$r = 25$

$I_o(r) = 0.62$

Min. rms location error = 0.4 μ

A number of other images with various degrees of exposure on emulsions 103-F, 1-N, and 103a-U were analyzed in the same manner and the results were similar, i.e., near (subjective) threshold the minimum rms position error is about 2 microns and this error becomes progressively less as the exposure is increased, but not to the point of saturation. It is possible that other sources of error[18] will exceed 1 micron so that an intrinsic limit of 1 to 2 microns will not, in general, seriously degrade overall location error.

In the above example, σ_x is much larger for the threshold image than for the well-developed one. This is contrary to what one might expect since it is well known that a point image spreads as the exposure increases. The reason for the larger σ_x is that the threshold images have to be smoothed by averaging over a large area in order to obtain a reasonably symmetrical, bell-shaped density profile for which the analysis applies. This can be seen by reference to Fig. 23 (or Fig. 19) and 24. Smoothing was accomplished in this instance by the use of a planimeter on the densitometer traces of Fig. 23.

A precaution should be noted with regard to the quantitative results obtained in this section. Photographic emulsions are known to differ significantly from one lot to another; therefore the results obtained herein may differ to some extent from those obtained with other plates of the same emulsion types.

SECTION 4

CONCLUSIONS

Conclusions drawn from this study are as follows:

(1) Approximately 1.5×10^5 photons at 6940Å within a 50-μ diameter area are required for the reliable and non-ambiguous detection of the resulting image on spectroscopic emulsion Type 103-F.† This assumes pre-exposure of the emulsion, or its exposure to background radiation, so that the gross background density in the vicinity of the image is about 0.3 to 0.4. [At the toe of the characteristic function, pre-exposure increases the emulsion sensitivity, which is proportional to increment of developed density/increment of exposure, much faster than it increases the noise, which is proportional to σ (average background density)]. This also assumes detection by a statistically significant increase in density when scanned by a microdensitometer having a 50-μ diameter aperture.

(2) The exposure energy requirement will be approximately doubled if pre-exposure, or its equivalent, is not used.

(3) The exposure energy will probably have to be increased by an additional factor of about 1.5 if detection is by visual examination, augmented with optical magnification of from 250X to 450X.†† This has not been demonstrated rigorously because of insufficient data; however, it is reasonable to expect that the psycho-physical system of human vision cannot as effectively perform the averaging operation required to detect a minimal image in a background of noise

† The energy at the camera aperture would have to be 20% greater due to diffraction losses; other losses due to optical attenuation should be taken into account.

†† Without such magnification the visual detection of threshold images is very difficult, if not impossible.

(4) The nominal expected image area is an appropriate microdensitometer aperture when searching for an image near the threshold limit of detection. (Smaller scanning areas result in an increase of the rms noise, $\approx 1/$ (aperture area)$^{1/2}$, without a proportional increase in the peak density of the image.)

(5) The intrinsic image location error will vary from a minimum rms value of about 0.5 micron for a well-exposed image to about 2 microns for threshold images in which the signal energy is confined to a 50-micron-diameter area.

(6) Failure of the reciprocity law and the exposure-intermittency effect are not significant for emulsion 103-F under the usual conditions of geodetic laser photography.

(7) The scintillation effect due to the optical "roughness" of the target is not significant because of the large number of output pulses from a laser operating in the normal mode. (The returns from these pulses are integrated in a common image area by the photographic emulsion, and each return constitutes a statistically independent detection trial.)

(8) Detection by developed-grain count does not appear to be either practical or advantageous at the density levels where detection sensitivity is optimum.

(9) The conclusions (1) through (8) apply in a general way to spectroscopic emulsions 103a-U and 1-N; optimum pre-exposure will be different.

SECTION 5

RECOMMENDATIONS FOR FUTURE WORK

The following programs are recommended as a course of future work:

(1) Evaluation of prospective new emulsions for geodetic satellite photography, using the principles and methods described in this report.

(2) Provide means to pre-expose plates used for geodetic satellite photography, if this is necessary for optimum sensitivity.

(3) Experimental study of microdensitometer search for threshold images, and comparison of this mode of detection with visual detection.

APPENDIX

SAMPLE CALCULATION OF $\sigma(\bar{D})$

Emulsion: 103-F, Plate No. 3 (See Table 1)

Sample No.	D(40X)	D^2(1600X)	Sample No.	D(40X)	D^2(1600X)
1	8.0	64.00	41	6.5	42.25
2	5.3	28.09	42	5.0	25.00
3	4.8	23.04	43	6.0	36.00
4	5.5	30.25	44	5.1	32.49
5	5.4	29.16	45	6.3	39.69
6	6.9	47.61	46	6.0	36.00
7	6.7	44.89	47	6.2	38.44
8	6.3	39.69	48	6.0	36.00
9	6.6	43.56	49	4.8	23.04
10	6.0	36.00	50	6.9	47.61
11	6.9	47.61	51	7.0	49.00
12	6.0	36.00	52	7.5	56.25
13	8.0	64.00	53	7.2	51.84
14	5.9	34.81	54	7.0	49.00
15	4.7	22.09	55	6.0	36.00
16	6.0	36.00	56	5.8	33.64
17	5.8	33.64	57	6.9	47.61
18	5.4	29.16	58	7.0	49.00
19	7.5	56.25	59	5.5	30.25
20	7.4	54.76	60	5.1	26.01
21	7.3	53.29	61	6.0	36.00
22	7.0	49.00	62	5.5	30.25
23	6.9	47.61	63	5.2	27.04
24	6.3	39.69	64	5.0	25.00
25	7.2	51.84	65	7.7	59.29
26	8.0	64.00	66	7.0	49.00
27	6.9	47.61	67	7.4	54.76
28	6.0	36.00	68	6.0	36.00
29	7.6	57.76	69	5.9	34.81
30	6.5	42.25	70	5.6	31.36
31	5.5	30.25	71	7.6	57.76
32	5.9	34.81	72	6.3	39.69

Sample No.	D(40X)	D^2(1600X)	Sample No.	D(40X)	D^2(1600X)
33	5.5	30.25	73	6.4	40.96
34	5.7	32.49	74	6.6	43.56
35	6.5	42.25	75	4.8	23.04
36	5.2	27.04	76	5.3	28.09
37	6.4	40.96	77	5.2	27.04
38	6.3	39.69	78	5.8	33.64
39	7.9	62.41	79	6.5	42.25
40	6.9	47.61	80	6.1	37.21
Σ	256.6	1,677.42	Σ	246.3	1,542.87

$$\bar{D} = \frac{502.9}{40 \times 80} = 0.1572$$

$$\overline{D^2} = \frac{3220}{1600 \times 80} = 0.02516$$

$$\sigma(\bar{D}) = \sqrt{\overline{D^2} - \bar{D}^2} = \sqrt{0.02516 - 0.02471} = 0.021$$

REFERENCES

1. Helmick, P. S., "On the Quantity of Light Energy Required to Render Developable a Grain of Silver Bromide," Vol. 5, J. Opt. Soc. Am., 1922, pp. 998-1015.

2. Sheppard, S. F., "The Formation of the Photographic Latent Image," Vol. 68, Phot. J., 1928, pp. 397-415.

3. James, T. H., and Higgins, G. C., Fundamentals of Photographic Theory, 2nd Edition, Morgan and Morgan, Inc., New York, N. Y., 1960.

   a. Chap. 3
   b. Chap. 4
   c. Chap. 13
   d. pp. 298-309
   e. Chap. 11
   f. pp. 266-281
   g. pp. 72-73

4. Mees, C. E. K., The Theory of the Photographic Process, Revised Edition, The MacMillan Co., New York, N. Y., 1954.

   a. Chap. 4 and 5
   b. Chap. 6 and 7
   c. Chap. 5
   d. pp. 981-1000
   e. pp. 213-221

5. Silberstein, L., "Contribution to the Theory of Photographic Exposure," Vol. 5, Phil. Mag., 1928, pp. 464-489.

6. Webb, J. H., "Number of Quanta Required to Form the Photographic Latent Image as Determined from Mathematical Analysis of the H and D Curve," Vol. 29, J. Opt. Soc. Am., 1939, pp. 309-313.

7. Silberstein, L., "On the Number of Quanta Required for the Developability of a Silver Halide Grain," Vol. 31, J. Opt Soc. Am., 1941, pp. 343-348.

8. Webb, J. H., "Number of Quanta Required to Form the Photographic Latent Image as Determined from Mathematical Analysis of the H and D Curve," Vol. 31, J. Opt. Soc. Am., 1941, pp. 348-354.

9. Zweig, H. J., "Theoretical Considerations on the Quantum Efficiency of Photographic Detectors," Vol. 51, No. 3, J. Opt. Soc. Am., March 1961, pp. 310-318.

10. Zweig, H. J., Higgins, G. C., and Mac Adam, D. L., "On the Information-Detecting Capacity of Photographic Emulsions," Vol. 48, No. 12, J. Opt. Soc. Am., December 1958.

a. pp. 926-933 b. p. 931

11. Zweig, H. J., "Autocorrelation and Granularity, Part I, Theory," and "Autocorrelation and Granularity, Part II, Results on Flashed Black-and-White Emulsions," Vol. 46, No. 10, J. Opt. Soc. Am., October 1956, pp. 805-820.

12. O' Neill, E. L., Introduction to Statistical Optics, Addison-Wesley Publishing Co., Inc., Reading, Mass., 1963.

a. Chap. 7 b. pp. 20-27

13. Zweig, H. J., "The Relation of Quantum Efficiency to Energy-and-Contrast-Detectivity for Photographic Materials," Vol. 5, No. 3, Phot. Sc. and Eng., May-June 1961, p. 142.

14. Jones, R. C., "On the Quantum Efficiency of Photographic Negatives," Vol. 2, Phot. Sc. and Eng., August 1958, pp. 57-65.

15. Branscomb, L. M., "Criteria for Pre-Exposure of Spectroscopic Plates," Vol. 41, No. 4, J. Opt. Soc. Am., April 1951, pp. 255-260.

16. Ackerman, S., and Morrison, T. S., "Study of a Multi-Pulse Laser Range Finder," AFCRL-66-755, 20 October 1966.

17. Webb, J. H., "Relationship Between Reciprocity-Law Failure and the Intermittency Effect in Photographic Exposure," Vol. 23, J. Opt. Soc. Am., 1933.

18. Farrell, E. J., "Intrinsic Limitations in Locating Photographic Star Images," Vol. 56, No. 10, J. Opt. Soc. Am., October 1966, pp. 1385-1390.

19. Farrell, E. J., "Information Content of Photoelectric Star Images," Vol. 56, No. 5, J. Opt. Soc. Am., May 1966, pp. 578-587.

BIBLIOGRAPHY

Altman, J. H., and Zweig, H. J., "Effects of Spread Function on the Storage of Information on Photographic Emulsions," Vol. 7, No. 3, Phot. Sc. and Eng., May-June 1963, pp. 173-177.

Haugh, E. F., "Theory for Optical Density and Developed Silver as Functions of Exposure," Vol. 6, No. 6, Phot. Sc. and Eng., December 1962, pp. 370-375.

Helmick, P. S., "The Average Quantity of Ultraviolet Light Energy Required to Render Developable a Grain of Photographic Silver Bromide," Vol. 9, J. Opt. Soc. Am., 1924, pp. 521-539.

James, T. H., and Coleman, J. J., "Quantum Theory of the Latent Photographic Image," Vol. 2, J. Chem. Phys., 1934, pp. 483-487.

Jones, R. C., "Information Capacity of Photographic Films," Vol. 51, No. 11, J. Opt. Soc. Am., November 1961, pp. 1159-1171.

Marchant, J. C., "Exposure Criteria for the Photographic Detection of Threshold Signals," Vol. 54, No. 6, J. Opt. Soc. Am., June 1964, pp. 798-800.

Marchant, J. C., and Millikan, A. G., "Photographic Detection of Faint Stellar Objects," Vol. 55, No. 8, J. Opt. Soc. Am., August 1965, pp. 907-911.

Selwyn, W. H., "Number of Quanta Required to Form the Photographic Latent Image as Determined from Mathematical Analysis of the H and D Curve," Vol. 29, J. Opt. Soc. Am., 1939, p. 518.

Unclassified

Security Classification

DOCUMENT CONTROL DATA - R&D

(Security classification of title, body of abstract and indexing annotation must be entered when the overall report is classified)

1. ORIGINATING ACTIVITY (Corporate author)	2a. REPORT SECURITY CLASSIFICATION
EG&G, Inc. Crosby Drive Bedford, Massachusetts	Unclassified 2b. GROUP

3. REPORT TITLE

THRESHOLD DETECTION OF GEODETIC SATELLITE IMAGES

4. DESCRIPTIVE NOTES (Type of report and inclusive dates)

Scientific Report (Interim)

5. AUTHOR(S) (Last name, first name, initial)

Ackerman, Sumner (NMI)

6. REPORT DATE	7a. TOTAL NO. OF PAGES	7b. NO. OF REFS
21 November 1966	60	20

8a. CONTRACT OR GRANT NO.	9a. ORIGINATOR'S REPORT NUMBER(S)
AF 19(628)-5516 b. PROJECT NO. and Task No. 7600-06 c. Element No. 62405394 d. Sub-Element No. 681000	EG&G Report No. B-3455 Scientific Report No. 3 9b. OTHER REPORT NO(S) (Any other numbers that may be assigned this report) AFCRL-67-0034

10. AVAILABILITY/LIMITATION NOTICES

Distribution of this document is unlimited.

11. SUPPLEMENTARY NOTES	12. SPONSORING MILITARY ACTIVITY
	Hq. AFCRL, OAR (CRJ) United States Air Force 01730 L. G. Hanscom Field, Bedford, Mass.

13. ABSTRACT

A literature survey and study has been made on the photographic detection of stellar images. Photographic detection theory in the literature has been extended as required by the special conditions of geodetic satellite photography. These conditions include the optical and temporal characteristics of the laser illumination, the optical roughness of the satellite reflector, and the quality of detection desired.

Experimental work was conducted to determine the energy requirements and the intrinsic location error for threshold images on Type 103-F emulsion. The energy required was found to be 1.5×10^5 to 4.5×10^5 photons at 6940Å; the lower figure applied to objective detection with a microdensitometer having an aperture area equal to the nominal area of the image and requires optimum pre-exposure of the emulsion. The minimum rms location error varies from about 0.5 micron for well-exposed images (exposed over an area of 50-microns diameter) to 2 microns for threshold images.

Failure of the reciprocity law, the effect of intermittent exposure, and scintillation due to the optically rough reflector are not significant. The basic results obtained for emulsion Type 103-F apply essentially to spectroscopic emulsions Types 1-N and 103a-U also.

DD FORM 1 JAN 64 1473

Unclassified

Security Classification

14. KEY WORDS	LINK A		LINK B		LINK C	
	ROLE	WT	ROLE	WT	ROLE	WT
Lasers Geodesy Satellites Illuminators Photography						

INSTRUCTIONS

1. ORIGINATING ACTIVITY: Enter the name and address of the contractor, subcontractor, grantee, Department of Defense activity or other organization *(corporate author)* issuing the report.

2a. REPORT SECURITY CLASSIFICATION: Enter the overall security classification of the report. Indicate whether "Restricted Data" is included. Marking is to be in accordance with appropriate security regulations.

2b. GROUP: Automatic downgrading is specified in DoD Directive 5200.10 and Armed Forces Industrial Manual. Enter the group number. Also, when applicable, show that optional markings have been used for Group 3 and Group 4 as authorized.

3. REPORT TITLE: Enter the complete report title in all capital letters. Titles in all cases should be unclassified. If a meaningful title cannot be selected without classification, show title classification in all capitals in parenthesis immediately following the title.

4. DESCRIPTIVE NOTES: If appropriate, enter the type of report, e.g., interim, progress, summary, annual, or final. Give the inclusive dates when a specific reporting period is covered.

5. AUTHOR(S): Enter the name(s) of author(s) as shown on or in the report. Enter last name, first name, middle initial. If military, show rank and branch of service. The name of the principal author is an absolute minimum requirement.

6. REPORT DATE: Enter the date of the report as day, month, year; or month, year. If more than one date appears on the report, use date of publication.

7a. TOTAL NUMBER OF PAGES: The total page count should follow normal pagination procedures, i.e., enter the number of pages containing information.

7b. NUMBER OF REFERENCES: Enter the total number of references cited in the report.

8a. CONTRACT OR GRANT NUMBER: If appropriate, enter the applicable number of the contract or grant under which the report was written.

8b, 8c, & 8d. PROJECT NUMBER: Enter the appropriate military department identification, such as project number, subproject number, system numbers, task number, etc.

9a. ORIGINATOR'S REPORT NUMBER(S): Enter the official report number by which the document will be identified and controlled by the originating activity. This number must be unique to this report.

9b. OTHER REPORT NUMBER(S): If the report has been assigned any other report numbers *(either by the originator or by the sponsor)*, also enter this number(s).

10. AVAILABILITY/LIMITATION NOTICES: Enter any limitations on further dissemination of the report, other than those imposed by security classification, using standard statements such as:

(1) "Qualified requesters may obtain copies of this report from DDC."

(2) "Foreign announcement and dissemination of this report by DDC is not authorized."

(3) "U. S. Government agencies may obtain copies of this report directly from DDC. Other qualified DDC users shall request through _____."

(4) "U. S. military agencies may obtain copies of this report directly from DDC. Other qualified users shall request through _____."

(5) "All distribution of this report is controlled. Qualified DDC users shall request through _____."

If the report has been furnished to the Office of Technical Services, Department of Commerce, for sale to the public, indicate this fact and enter the price, if known.

11. SUPPLEMENTARY NOTES: Use for additional explanatory notes.

12. SPONSORING MILITARY ACTIVITY: Enter the name of the departmental project office or laboratory sponsoring *(paying for)* the research and development. Include address.

13. ABSTRACT: Enter an abstract giving a brief and factual summary of the document indicative of the report, even though it may also appear elsewhere in the body of the technical report. If additional space is required, a continuation sheet shall be attached.

It is highly desirable that the abstract of classified reports be unclassified. Each paragraph of the abstract shall end with an indication of the military security classification of the information in the paragraph, represented as *(TS), (S), (C), or (U)*.

There is no limitation on the length of the abstract. However, the suggested length is from 150 to 225 words.

14. KEY WORDS: Key words are technically meaningful terms or short phrases that characterize a report and may be used as index entries for cataloging the report. Key words must be selected so that no security classification is required. Identifiers, such as equipment model designation, trade name, military project code name, geographic location, may be used as key words but will be followed by an indication of technical context. The assignment of links, rules, and weights is optional.